Minimum Time Observer Designs for $n + m$ Linear Hyperbolic Systems with Unilateral, Bilateral or Pointwise In-Domain Sensing

Nils Christian A. Wilhelmsen[a,*], Henrik Anfinsen[b], Ole Morten Aamo[b]

[a] *Centre Automatique et Systèmes, MINES ParisTech, PSL Research University, 75006 Paris, France*
[b] *Department of Engineering Cybernetics, Norwegian University of Science and Technology, Trondheim N-7491, Norway*

Abstract

In this paper we derive minimum time convergent observers for $n + m$[1] systems of linear coupled first-order 1-D hyperbolic PDEs, that use either unilateral (single boundary measured), bilateral (both boundaries measured) or pointwise in-domain sensing. First, a Volterra integral transformation is combined with a Fredholm integral transformation to derive a minimum time unilateral observer for $n + m$ systems. Then, it is shown that an $n + m$ system with bilateral sensing can be transformed to an $(n + m) + (n + m)$ system with unilateral sensing via an invertible coordinate transformation. The $n + m$ bilateral observer is subsequently obtained from the $(n + m) + (n + m)$ minimum time unilateral observer, and it is shown that it converges in a theoretical minimum time for bilateral sensing. In a similar fashion, the observer using pointwise in-domain measurement is derived using the same techniques. The performances of the $n + m$ bilateral and unilateral observers are demonstrated in simulations.

Keywords: Observer design, Hyperbolic PDEs, Backstepping
2020 MSC: 93C20

1. Introduction

1.1. Problem statement

We are interested in systems with dynamics given by

$$u_t(x,t) + \Lambda^+ u_x(x,t) = \Sigma^{++}(x)u(x,t) + \Sigma^{+-}(x)v(x,t) \tag{1a}$$
$$v_t(x,t) - \Lambda^- v_x(x,t) = \Sigma^{-+}(x)u(x,t) + \Sigma^{--}(x)v(x,t) \tag{1b}$$
$$u(0,t) = Q_0 v(0,t) + U_0(t) \tag{1c}$$
$$v(1,t) = R_1 u(1,t) + U_1(t) \tag{1d}$$
$$u(x,0) = u_0(x) \tag{1e}$$
$$v(x,0) = v_0(x) \tag{1f}$$

where

$$u(x,t) := [u_1(x,t), \dots, u_n(x,t)]^\top, \tag{2a}$$
$$v(x,t) := [v_1(x,t), \dots, v_m(x,t)]^\top \tag{2b}$$

are the states defined over $x \in [0,1]$, $t \in [0,\infty)$, and $n, m \in \mathbb{Z}$, satisfying $n, m \geq 1$.

The transport speed matrices

$$\Lambda^+ := \operatorname{diag}\{\lambda_1, \dots, \lambda_n\}, \tag{3a}$$
$$\Lambda^- := \operatorname{diag}\{\mu_1, \dots, \mu_m\} \tag{3b}$$

have components subject to the restriction,

$$-\mu_m < \cdots < -\mu_1 < 0 < \lambda_1 < \cdots < \lambda_n \tag{4}$$

and the coupling coefficient matrices

$$\Sigma^{++}(x) := \{\sigma^{++}_{ij}(x)\}_{1\leq i,j\leq n} \tag{5a}$$
$$\Sigma^{+-}(x) := \{\sigma^{+-}_{ij}(x)\}_{1\leq i\leq n, 1\leq j\leq m} \tag{5b}$$
$$\Sigma^{-+}(x) := \{\sigma^{-+}_{ij}(x)\}_{1\leq i\leq m, 1\leq j\leq n} \tag{5c}$$
$$\Sigma^{--}(x) := \{\sigma^{--}_{ij}(x)\}_{1\leq i,j\leq m} \tag{5d}$$

have components satisfying $\sigma^{++}_{ij}, \sigma^{+-}_{ij}, \sigma^{-+}_{ij}, \sigma^{--}_{ij} \in L^\infty((0,1);\mathbb{R})$. Also, it is assumed without loss of generality that the diagonal entries satisfy $\sigma^{++}_{ii} = \sigma^{--}_{jj} = 0$ (see the coordinate transformation considered in [1]). The reflection coefficient matrices

$$Q_0 := \{q_{ij}\}_{1\leq i\leq n, 1\leq j\leq m} \tag{6a}$$
$$R_1 := \{\rho_{ij}\}_{1\leq i\leq m, 1\leq j\leq n} \tag{6b}$$

have components satisfying $q_{ij}, \rho_{ij} \in \mathbb{R}$, and we assume the boundary inputs $U_0 \in C^0([0,\infty);\mathbb{R}^n)$ and $U_1 \in C^0([0,\infty);\mathbb{R}^m)$.

We consider in this paper weak solutions of (1). That is, we take as the weak solution to (1) the solution of the corresponding integral equation resulting from multiplying (1) by sufficiently smooth test functions and integrating by parts. It can be shown (see Theorem A.4 in [2]) that for initial condition $u_0 \in L^2((0,1);\mathbb{R}^n), v_0 \in L^2((0,1);\mathbb{R}^m)$, (1) has a unique (weak) solution $u \in C^0([0,\infty);L^2((0,1);\mathbb{R}^n)), v \in$

⋆A less general version of the material in this paper was presented at the 18th European Control Conference (ECC), June 25-28, 2019, Naples, Italy.

*Corresponding author
Email addresses: nils.wilhelmsen@mines-paristech.fr (Nils Christian A. Wilhelmsen), henrik.anfinsen@ntnu.no (Henrik Anfinsen), aamo@ntnu.no (Ole Morten Aamo)

[1] By the phrase "$n+m$ hyperbolic system" (or just "$n+m$ system") we mean a hyperbolic PDE consisting of $n + m$ coupled equations, for which n transport speeds are positive and m transport speeds are negative. Such systems are often referred to as "$p \times p$ systems" in the literature (with $p = n + m$).

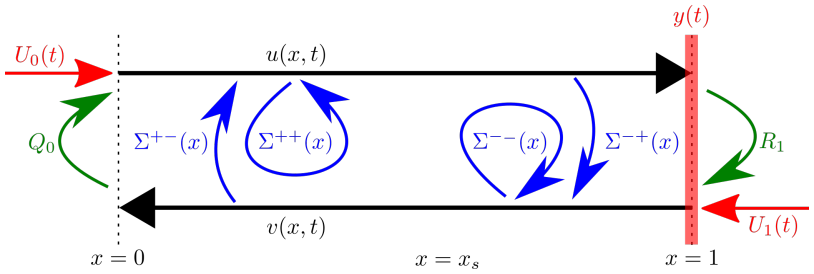

(a) **Scenario 1:** The measurement signal, represented by y, is taken at a single boundary. The case of sensing at $x = 1$ is shown.

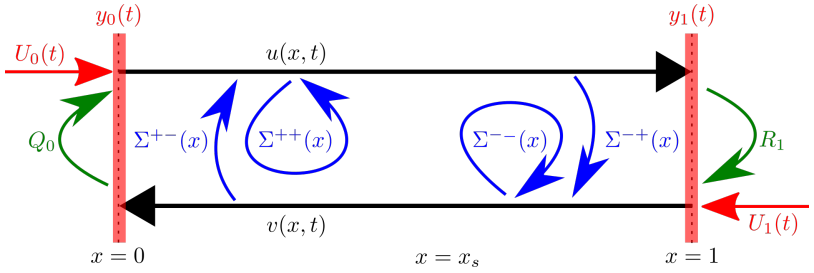

(b) **Scenario 2:** Sensing occurs at both boundaries, $x = 0$ and $x = 1$, resulting in respective output signals y_0 and y_1.

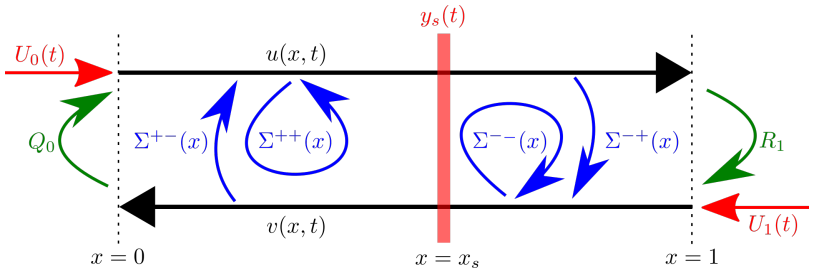

(c) **Scenario 3:** Sensing is performed at a single in-domain point $x = x_s$, resulting in the output signal y_s.

Figure 1: Schematics of the system (1) representing the three sensing scenarios considered in this paper. The black arrows represent the distributed vector states u, v, respectively drawn as single arrows for ease of viewing. The green arrows represent the boundary reflection coefficient matrices Q_0, R_1, the blue arrows denote the internal coupling coefficient matrix valued functions $\Sigma^{++}, \Sigma^{+-}, \Sigma^{-+}, \Sigma^{--}$, and the red arrows denote boundary input signals U_0, U_1. The position where sensing is performed is illustrated by vertical red bars, accompanied by the resultant output signal, in the three diagrams.

$C^0([0,\infty); L^2((0,1); \mathbb{R}^m))$. Some further details are given in Appendix B.

In many applications involving hyperbolic PDE systems, it is desirable to know the numerical value of the state vectors (u, v) across the domain as the process evolves, either for general monitoring or control purposes. However, distributed sensing across the domain can in certain cases be expensive or even infeasible. An example application of this is oil well drilling, where the actuation and sensing equipment is typically located on the rig [3], but the drill string one is interested in monitoring and controlling stretches downhole for several kilometres. This should motivate reconstructing the states of hyperbolic PDE systems from boundary measurements, and to do this one can design state observers, a concept first introduced for lumped, linear systems in [4].

In this paper, we wish to design observers for the $n + m$ system (1) that produce state estimates $(\hat{u}, \hat{v})$ which converge to the correct system states (u, v) in finite time. Following a line of research that attempts to characterize the duration of time controllability and observability objectives can be achieved within for hyperbolic PDE systems, some notable contributions being [5] and [6], in [7] the existence of boundary observers for $n + m$ linear hyperbolic systems able to estimate the state exactly within a given finite time is proven. This finite time is equal to the sum of propagation times over the spatial domain of the slowest characteristic in each direction, if a single boundary is measured, and the propagation time of the slowest characteristic overall, if both boundaries are measured. In this paper, we say that an observer is *minimum time* convergent if it is able to achieve one of these two convergence times proven to be achievable in [7], depending on the measurement data available. If, on the other hand, an observer requires a larger time to produce correct estimates than a minimum time convergent observer, given the same amount of data, we refer to it as a *non-minimum time* convergent observer.

We consider only pointwise measurements, so distributed sensing is outside the scope of this paper. In total, three cases are considered (see Figure 1):

1. Sensing taken at a single boundary only, so either $v(0,\cdot)$ or $u(1,\cdot)$ is known. The output signal is for this scenario denoted y.
2. Sensing taken at both boundaries, so both $v(0,\cdot)$ and $u(1,\cdot)$ are known. The output signals are here denoted y_0 and y_1, respectively.

3. Sensing taken at an internal point $x_s \in (0,1)$, so $(u(x_s,\cdot), v(x_s,\cdot))$ is known. For this scenario we denote the output signal as y_s.

For Case 1, the theoretical lower bound $t_{1,min}$ for convergence time possible to achieve is defined in [7] as

$$t_{1,min} := \frac{1}{\lambda_1} + \frac{1}{\mu_1}. \tag{7}$$

However, for Cases 2 & 3, a strictly smaller theoretical lower bound $t_{2,min}$ for convergence time is possible to achieve, also defined in [7] as

$$t_{2,min} := \max\left\{\frac{1}{\lambda_1}, \frac{1}{\mu_1}\right\}. \tag{8}$$

Remark 1.1. *It should be noted that by minimum convergence time for Case 1 we refer in this paper, as has been done previously in the literature (see e.g. [8, 9]), to the lowest convergence time that can be guaranteed given Λ^+, Λ^-, uniformly with respect to the remaining parameters, Σ^{++}, Σ^{+-}, Σ^{-+}, Σ^{--}, Q_0 and R_1. In other words, there may be specific Σ^{++}, Σ^{+-}, Σ^{-+}, Σ^{--}, Q_0 and R_1 that allow a shorter convergence time. The easiest way to see this is the case where these parameters are zero. A copy (observer) of* (1a), (1c) *will converge to the state of the plant in time $\frac{1}{\lambda_1}$ and a copy of* (1b), (1d) *will converge to the state of the plant in time $\frac{1}{\mu_1}$. Thus, the state can be observed in time $\max\left\{\frac{1}{\lambda_1}, \frac{1}{\mu_1}\right\} < t_{1,min}$ in this particular case.*

An observer that produces estimates of (1) within the minimum time (7) for single-boundary sensing is published in [8], but when used together with a full-state feedback law to produce an output-feedback controller, the control input must be anti-collocated with the sensed boundary. This partially solves Case 1, but it is beneficial in practice to also have the option of applying collocated measurement and control. The observer given in [10] allows the sensor to be collocated to the actuator, but the convergence time is

$$t_{1,nonmin} := \sum_{i=1}^{n} \frac{1}{\lambda_i} + \frac{1}{\mu_1} \tag{9}$$

which is larger than (7) for systems with $n > 1$. This paper builds on the observer from [10] by proposing an observer converging in minimum time (7) that can be used with a collocated boundary control signal, fully solving Case 1.

The problem posed by Case 2 is solved in [11] by introducing the adjoint control system and defining the observer in terms of it. This paper, however, takes an alternate route and generalizes the work in [9] to the $n + m$ case.

1.2. Background

Systems of coupled first-order linear hyperbolic PDEs, along with their observation and control problems, have recently been subject to research due to their application in modeling various physical scenarios. A comprehensive overview of recent progress is given in [2]. Applications include heat exchangers [12], gas pipelines [13] and oil well drilling [14], to name a few. A gradually more common method for observer and controller design for this type of systems is the infinite dimensional backstepping method, initially pioneered for parabolic PDE control design in [15], and subsequently appearing in its fully infinite dimensional form in [16]. Applying the backstepping method for observer design was first seen for parabolic PDEs in [17], where an observer that converges to the origin exponentially in the L^2 and H^1 norms is given. Although an exponential convergence rate is sufficient for a wide range of applications, in certain scenarios stronger convergence guarantees, such as *finite* or even *prescribed* time convergence, are required. Initially investigated for finite-dimensional systems [18, 19, 20], finite [21] and prescribed [22, 23] time stabilization of parabolic PDEs has been researched as of late.

For hyperbolic PDEs, achieving finite time convergence is more natural, and in [24] the first controller and observer for 2×2 hyperbolic systems (same as (1), but with $n = m = 1$) is presented, resulting in a boundary output-feedback controller where sensing and actuation is collocated. Building on the finite but non-minimum time convergent observer in [10], that enables implementation of collocated output-feedback control for $n + m$ systems, the $2 + 2$ system observer designed in [9] modifies the observer from [10] by changing the non-minimum time convergent target system used there to be minimum time convergent. This is done with the help of a Fredholm integral transformation, following ideas from [25], [11]. Expressions for 2×2 bilateral observer gains using a domain folding trick similar to the one suggested in [26] for stabilization of systems of reaction-diffusion equations, are then derived. This paper takes a similar strategy to that of [9], generalizing the results to the $n + m$ setting.

Here we proceed by designing the single boundary observer first (Case 1), before using this result to design the observers for bilateral sensing (Case 2) and pointwise in-domain sensing (Case 3). The single boundary observer is designed with the help of two transformations, first a *Volterra transformation* mapping it into an *intermediate target system*, and secondly a *Fredholm transformation* mapping the intermediate target system into a *final target system*. The mapping between the intermediate and final target systems allows the calculation of an "artificial observer gain", T^+. Likewise, the mapping between the system with single boundary sensing and the intermediate target system produces observer gains P^+, P^-, which in turn depend on T^+ to achieve minimum time convergence. Next, for Cases 2 & 3, the systems considered are "folded" into a system with single boundary measurement, allowing the observer designed for Case 1 to be applied. The resultant observer gains, $P^{++}, P^{+-}, P^{-+}, P^{--}$ for Case 2 and P_s^+, P_s^- for Case 3, can then be computed based on the corresponding P^+, P^- by "folding" back. A schema giving an overview over the transformations considered and corresponding gains is in Figure 2.

This paper is organized as follows. Section 2 presents the unilateral observer design for $n + m$ systems, and the result is applied in Section 3 to obtain the minimum time observers for bilateral and pointwise in-domain sensing. Results from a simulation are given in Section 4 before some concluding remarks

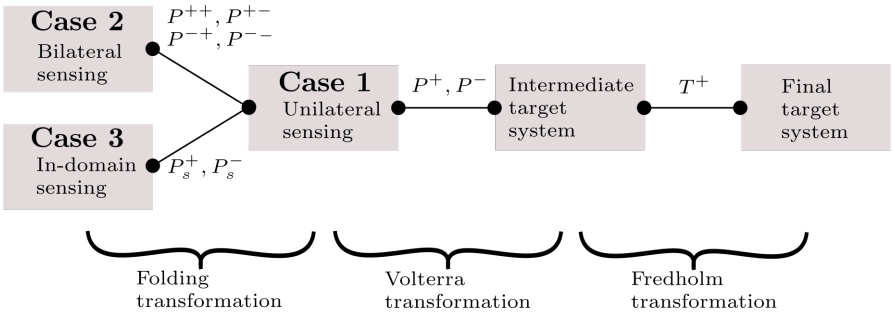

Figure 2: Schema with overview over systems and transformations considered in this paper.

are offered in Section 5.

2. Minimum time observer with unilateral sensing

2.1. Problem statement

Within the scope of this section we assume a single boundary of (1) is measured, only, and without loss of generality (due to the symmetry of (1)) assume the measurement is

$$y(t) := u(1,t), \tag{10}$$

with $y = [y_1, \dots, y_n]^\top$ being a vector. The term $u(1,\cdot)$ appearing in (10) is here interpreted as the corresponding term appearing (see (B.1) in Appendix B) when defining the solution of (1). Using knowledge of this output signal, in addition to possible input signals U_0, U_1, we would like to produce state estimates $(\hat{u}, \hat{v}) \to (u, v)$ in finite time $t_{1,min}$ given by (7).

To achieve this, we propose here the observer

$$\begin{aligned}
\hat{u}_t(x,t) + \Lambda^+ \hat{u}_x(x,t) &= \Sigma^{++}(x)\hat{u}(x,t) + \Sigma^{+-}(x)\hat{v}(x,t) \\
&\quad + P^+(x)\left(y(t) - \hat{u}(1,t)\right) && \text{(11a)} \\
\hat{v}_t(x,t) - \Lambda^- \hat{v}_x(x,t) &= \Sigma^{-+}(x)\hat{u}(x,t) + \Sigma^{--}(x)\hat{v}(x,t) \\
&\quad + P^-(x)\left(y(t) - \hat{u}(1,t)\right) && \text{(11b)} \\
\hat{u}(0,t) &= Q_0 \hat{v}(0,t) + U_0(t) && \text{(11c)} \\
\hat{v}(1,t) &= R_1 y(t) + U_1(t) && \text{(11d)} \\
\hat{u}(x,0) &= \hat{u}_0(x) && \text{(11e)} \\
\hat{v}(x,0) &= \hat{v}_0(x) && \text{(11f)}
\end{aligned}$$

taking the form of the output-error injection observer given in Definition 5.3.1 of [27], represented in that text by an abstract operator differential equation and referred to as a *Luenberger observer*. The observer is initialized by $\hat{u}_0 \in L^2((0,1);\mathbb{R}^n)$ and $\hat{v}_0 \in L^2((0,1);\mathbb{R}^m)$. As for (1), it can be shown (see Theorem A.4 in [2]) that with this initial condition and observer gains assigned as presented below, (11) has a unique (weak) solution $\hat{u} \in C^0([0,\infty); L^2((0,1);\mathbb{R}^n))$, $\hat{v} \in C^0([0,\infty); L^2((0,1);\mathbb{R}^m))$.

The observer provides vector state estimates $\hat{u} = [\hat{u}_1, \dots, \hat{u}_n]^\top$ and $\hat{v} = [\hat{v}_1, \dots, \hat{v}_m]^\top$ by copying the plant dynamics (1), but additionally adding correction terms consisting of the spatially varying observer gains

$$P^+(x) := M(x,1)\Lambda^+ + T^+(x) + \int_x^1 M(x,\xi)T^+(\xi)d\xi \tag{12a}$$

$$P^-(x) := N(x,1)\Lambda^+ + \int_x^1 N(x,\xi)T^+(\xi)d\xi \tag{12b}$$

multiplied by the output estimation error $(y(\cdot) - \hat{u}(1,\cdot))$. The gains are functions of matrix valued functions M, N, that are defined further down in (14), and the "artificial gain" T^+ that modifies the gains to allow the observer (11) to achieve convergence in minimum time (7). The "artifical gain" T^+ is given by

$$T^+(x) := K(x,1)\Lambda^+, \tag{13}$$

with K defined further down in (16). By setting $T^+ \equiv 0$ in (12) one obtains the observer gains used in [10], which result in (11) converging in non-minimum time (9).

Firstly the kernel PDEs for M, N are introduced, and subsequently the kernel PDEs for K are given. The $n \times n$ matrix-valued function $M = \{M_{ij}\}_{1\le i,j\le n}$ and $m \times n$ matrix-valued function $N = \{N_{ij}\}_{1\le i\le m, 1\le j\le n}$ in (12) are solutions to the kernel PDE

$$\begin{aligned}
\Lambda^+ M_x(x,\xi) + M_\xi(x,\xi)\Lambda^+ &= \Sigma^{++}(x)M(x,\xi) \\
&\quad + \Sigma^{+-}(x)N(x,\xi) && \text{(14a)} \\
-\Lambda^- N_x(x,x) + N_\xi(x,\xi)\Lambda^+ &= \Sigma^{-+}(x)M(x,\xi) \\
&\quad + \Sigma^{--}(x)N(x,\xi) && \text{(14b)} \\
M(x,x)\Lambda^+ - \Lambda^+ M(x,x) &= \Sigma^{++}(x) && \text{(14c)} \\
N(x,x)\Lambda^+ + \Lambda^- N(x,x) &= \Sigma^{-+}(x) && \text{(14d)} \\
Q_0 N(0,\xi) - M(0,\xi) &= H(\xi) && \text{(14e)} \\
M_{ij}(x,1) &= \frac{\sigma_{ij}^{++}(x)}{\lambda_j - \lambda_i}, \text{ if } 1 \le j < i \le n && \text{(14f)}
\end{aligned}$$

defined over the triangular domain $\mathcal{T} := \{(x,\xi) \mid 0 \le x \le \xi \le 1\}$. Appearing in the boundary condition (14e), $H = \{h_{ij}\}_{1\le i,j\le n}$ is a strictly lower triangular $n \times n$ matrix, with components defined as

$$h_{ij}(\xi) = \begin{cases} \sum_{k=1}^{m} q_{ik}N_{kj}(0,\xi) - M_{ij}(0,\xi), & \text{if } 1 \le j < i \le n, \\ 0, & \text{otherwise.} \end{cases} \tag{15}$$

Next, the $n \times n$ strictly lower triangular matrix-valued function $K = \{k_{ij}\}_{1\le i,j\le n}$ is the solution to

$$\begin{aligned}
\Lambda^+ K_x(x,\xi) + K_\xi(x,\xi)\Lambda^+ &= -K(x,1)\Lambda^+ K(1,\xi) && \text{(16a)} \\
K(x,0) &= 0 && \text{(16b)}
\end{aligned}$$

$$\begin{vmatrix} k_{21} & & & & & & \\ \downarrow & & & & & & \\ k_{31} & \leftarrow & k_{32} & & & & \\ \downarrow & & \downarrow & & & & \\ \vdots & & \ddots & \leftarrow & k_{n-1,n-2} & & \\ \downarrow & \ddots & & & \downarrow & & \\ k_{n1} & \leftarrow & \dots & \leftarrow & k_{n,n-2} & \leftarrow & k_{n,n-1} \end{vmatrix}$$

Figure 3: Dependency among elements k_{ij} in computing K

$$K(0,\xi) = H(\xi) + \int_0^1 H(s)K(s,\xi)ds \quad (16c)$$

defined over the square domain $\mathcal{S} := \{(x,\xi)|0 \le x \le 1, 0 \le \xi \le 1\}$. Note that due to the definition of H, a term appearing in the boundary condition (16c), via (15), the system (14) must be solved prior to (16).

Provided that (4) holds, well-posedness of (14)–(15) is ensured by Theorem 3.3 in [28] (see the transformation given in Appendix B of [10]), which guarantees the existence of a unique solution $M \in L^\infty(\mathcal{T}; \mathcal{M}_{n,n}(\mathbb{R}))$ and $N \in L^\infty(\mathcal{T}; \mathcal{M}_{m,n}(\mathbb{R}))$. Further, applying the method of characteristics, the solution to (16) can be computed explicitly for each component. We obtain that

$$k_{ij}(x,\xi) = \begin{cases} \psi_{ij}(x,\xi), & \text{if } \xi \ge \frac{\lambda_j}{\lambda_i}x \\ 0, & \text{if } \xi < \frac{\lambda_j}{\lambda_i}x \end{cases} \quad (17)$$

provided $(x,\xi) \in \mathcal{S}$, where

$$\psi_{ij}(x,\xi) = k_{ij}\left(0, \xi - \frac{\lambda_j}{\lambda_i}x\right) - \int_0^{\frac{x}{\lambda_i}} \left(\sum_{k=j+1}^{i-1} \lambda_k k_{ik}(\lambda_i s, 1) k_{kj}\left(1, \lambda_j z + \xi - \frac{\lambda_j}{\lambda_i}x\right)\right) dz \quad (18)$$

and $k_{ij}(0,\xi)$ is given by

$$k_{ij}(0,\xi) = h_{ij}(\xi) + \int_0^1 \sum_{k=j+1}^{i-1} h_{ik}(s)k_{kj}(s,\xi)ds. \quad (19)$$

Since Theorem 3.3 of [28] guarantees that the boundary traces of M and N are $L^\infty([0,1]; \mathcal{M}_{n,n}(\mathbb{R}))$ and $L^\infty([0,1]; \mathcal{M}_{m,n}(\mathbb{R}))$, respectively, we see the boundary data for K in (16c) inherits this regularity due to (15). Hence the solution of K with components explicitly given by (17)–(19) is uniquely defined and in $L^\infty(\mathcal{S}; \mathcal{M}_{n,n}(\mathbb{R}))$. The $(i,j)^{th}$ element of K only depends on the solution to elements $k_{j+1,j}, k_{j+2,j}, \dots, k_{i-1,j}$ and $k_{i,j+1}, k_{i,j+1}, \dots, k_{i,i-1}$, which are respectively the elements in the same column and row as k_{ij}, between itself and the elements in the subdiagonal. Therefore, the solution can be computed recursively starting with the subdiagonal elements $k_{j+1,j}$, $j \in \{1, n-1\}$, and moving diagonally downwards towards the left, until computing element k_{n1} last (see Figure 3).

Remark 2.1. *The theory presented in this Section can be generalized to systems with space-dependent transport speeds $\lambda_i, \mu_j \in C^1([0,1];\mathbb{R})$, $i \in \{1,\dots,n\}$, $j \in \{1,\dots,m\}$. Here the theoretical lower bound for convergence time is for Case* 1 *expressed by $t_{1,min} = \int_0^1 \frac{dx}{\lambda_1(x)} + \int_0^1 \frac{dx}{\mu_1(x)}$, whereas for Cases* 2 *&* 3 *it is given by $t_{2,min} = \max\left\{\int_0^1 \frac{dx}{\lambda_1(x)}, \int_0^1 \frac{dx}{\mu_1(x)}\right\}$. The calculations and expressions are slightly more complicated, but the overall steps remain the same. However, for simplicity, readability, and cohesiveness with the rest of the paper it is presented for systems with constant transport speeds.*

Next, we present a convergence result for the observer (11).

Theorem 2.2. *Consider system* (1) *with output vector* (10) *and the observer* (11). *If the output injection gains are selected as* (12)–(16)*, then for all times $t \ge t_{1,min}$, we have that $(\hat{u}(\cdot,t), \hat{v}(\cdot,t)) = (u(\cdot,t), v(\cdot,t))$.*

Subsections 2.2–2.3 are devoted to proving Theorem 2.2.

2.2. Volterra backstepping transformation

Define the estimation errors $\tilde{u} := u - \hat{u}$ and $\tilde{v} := v - \hat{v}$. The error dynamics are found from (1) and (11) as

$$\tilde{u}_t(x,t) + \Lambda^+\tilde{u}_x(x,t) = \Sigma^{++}(x)\tilde{u}(x,t) + \Sigma^{+-}(x)\tilde{v}(x,t) - P^+(x)\tilde{u}(1,t) \quad (20a)$$

$$\tilde{v}_t(x,t) - \Lambda^-\tilde{v}_x(x,t) = \Sigma^{-+}(x)\tilde{u}(x,t) + \Sigma^{--}(x)\tilde{v}(x,t) - P^-(x)\tilde{u}(1,t) \quad (20b)$$

$$\tilde{u}(0,t) = Q_0\tilde{v}(0,t) \quad (20c)$$

$$\tilde{v}(1,t) = 0 \quad (20d)$$

$$\tilde{u}(x,0) = \tilde{u}_0(x) \quad (20e)$$

$$\tilde{v}(x,0) = \tilde{v}_0(x). \quad (20f)$$

As for (1) and (11), it can be shown (see Theorem A.4 in [2]) that with initial condition $\tilde{u}_0 := u_0 - \hat{u}_0, \tilde{v}_0 := v_0 - \hat{v}_0$, (20) has a unique (weak) solution $\tilde{u} \in C^0([0,\infty); L^2((0,1);\mathbb{R}^n))$, $\tilde{v} \in C^0([0,\infty); L^2((0,1);\mathbb{R}^m))$. Some further details are given in Appendix B.

The proof of the following Lemma follows similar steps as the proof of Lemma 10 in [10], but is included here to show the details behind the new observer gains (12), which are different from those in [10] to accommodate minimum time convergence.

Lemma 2.3. *The invertible Volterra integral transformation*

$$\tilde{u}(x,t) = \tilde{\alpha}(x,t) + \int_x^1 M(x,\xi)\tilde{\alpha}(\xi,t)d\xi \quad (21a)$$

$$\tilde{v}(x,t) = \tilde{\beta}(x,t) + \int_x^1 N(x,\xi)\tilde{\alpha}(\xi,t)d\xi \quad (21b)$$

maps

$$\tilde{\alpha}_t(x,t) + \Lambda^+\tilde{\alpha}_x(x,t) = \Sigma^{+-}(x)\tilde{\beta}(x,t) - \int_x^1 D^+(x,\xi)\tilde{\beta}(\xi,t)d\xi - T^+(x)\tilde{\alpha}(1,t) \quad (22a)$$

$$\tilde{\beta}_t(x,t) - \Lambda^-\tilde{\beta}_x(x,t) = \Sigma^{--}(x)\tilde{\beta}(x,t) - \int_x^1 D^-(x,\xi)\tilde{\beta}(\xi,t)d\xi \tag{22b}$$

$$\tilde{\alpha}(0,t) = Q_0\tilde{\beta}(0,t) + \int_0^1 H(\xi)\tilde{\alpha}(\xi,t)d\xi \tag{22c}$$

$$\tilde{\beta}(1,t) = 0 \tag{22d}$$

$$\tilde{\alpha}(x,0) = \tilde{\alpha}_0(x) \tag{22e}$$

$$\tilde{\beta}(x,0) = \tilde{\beta}_0(x) \tag{22f}$$

with initial conditions $\tilde{\alpha}_0 \in L^2((0,1);\mathbb{R}^n)$ *and* $\tilde{\beta}_0 \in L^2((0,1);\mathbb{R}^m)$*, into* (20) *where* M *and* N *satisfy* (14) *and* $D^+ = \{d^+_{ij}\}_{1\le i\le n, 1\le j\le m}$*,* $D^- = \{d^-_{ij}\}_{1\le i,j\le m}$ *are solutions to the integral equations*

$$D^+(x,\xi) = M(x,\xi)\Sigma^{+-}(\xi) - \int_x^\xi M(x,s)D^+(s,\xi)ds \tag{23a}$$

$$D^-(x,\xi) = N(x,\xi)\Sigma^{+-}(\xi) - \int_x^\xi N(x,s)D^+(s,\xi)ds \tag{23b}$$

respectively.

Proof. Differentiating (21) with respect to time and space, substituting in the target error system (22), integrating by parts and combining with (20) we find

$$\begin{aligned}
&\tilde{u}_t(x,t) + \Lambda^+\tilde{u}_x(x,t) - \Sigma^{++}(x)\tilde{u}(x,t) - \Sigma^{+-}(x)\tilde{v}(x,t)\\
&\quad + P^+(x)\tilde{u}(1,t) = \left(M(x,x)\Lambda^+ - \Lambda^+M(x,x) - \Sigma^{++}(x)\right)\tilde{\alpha}(x,t)\\
&\quad + \int_x^1 \Big(\Lambda^+M_x(x,\xi) + M_\xi(x,\xi)\Lambda^+ - \Sigma^{++}(x)M(x,\xi)\\
&\quad - \Sigma^{+-}(x)N(x,\xi)\Big)\tilde{\alpha}(\xi,t)d\xi + \int_x^1 \Big(M(x,\xi)\Sigma^{+-}(\xi) - D^+(x,\xi)\\
&\quad - \int_x^\xi M(x,s)D^+(s,\xi)ds\Big)\tilde{\beta}(\xi,t)d\xi + \Big(P^+(x) - M(x,1)\Lambda^+\\
&\quad - T^+(x) - \int_x^1 M(x,\xi)T^+(\xi)d\xi\Big)\tilde{\alpha}(1,t) = 0,
\end{aligned} \tag{24}$$

and

$$\begin{aligned}
&\tilde{v}_t(x,t) - \Lambda^-\tilde{v}_x(x,t) - \Sigma^{-+}(x)\tilde{u}(x,t) - \Sigma^{--}(x)\tilde{v}(x,t)\\
&\quad + P^-(x)\tilde{u}(1,t) = \left(N(x,x)\Lambda^+ + \Lambda^-N(x,x) - \Sigma^{-+}(x)\right)\tilde{\alpha}(x,t)\\
&\quad + \int_x^1 \Big(\Lambda^-N_x(x,\xi) + N_\xi(x,\xi)\Lambda^+ - \Sigma^{-+}(x)M(x,\xi)\\
&\quad - \Sigma^{--}(x)N(x,\xi)\Big)\tilde{\alpha}(\xi,t)d\xi + \int_x^1 \Big(N(x,\xi)\Sigma^{+-}(\xi) - D^-(x,\xi)\\
&\quad - \int_x^\xi N(x,s)D^+(s,\xi)ds\Big)\tilde{\beta}(\xi,t)d\xi + \Big(P^-(x) - N(x,1)\Lambda^+\\
&\quad - \int_x^1 N(x,\xi)T^+(\xi)d\xi\Big)\tilde{\alpha}(1,t) = 0.
\end{aligned} \tag{25}$$

From (24) and (25) we obtain (12), the definitions of D^+ and D^- (23), the PDEs (14a)–(14b) and the first two boundary conditions (14c)–(14d). For the third boundary condition, set $x = 0$ in (21) and substitute this into (20c), then apply (22c) to obtain

$$\int_0^1 H(\xi)\tilde{\alpha}(\xi,t)d\xi = \int_0^1 \left(Q_0N(0,\xi) - M(0,\xi)\right)\tilde{\alpha}(\xi,t)d\xi \tag{26}$$

from which the required boundary condition (14e) trivially follows. Finally, (14f) is an additional boundary condition required for well-posedness, as was done in [28] for equations in the same form.

2.3. Fredholm integral transformation

Now a target system which converges in minimum time (7) is introduced, and proved to be equivalent with (20). Using K from (16), Σ^{+-} from (5) and D^+ from (23), define first an $n\times n$ matrix-valued function $\Phi = \{\phi_{ij}\}_{1\le i,j\le n}$ as

$$\begin{aligned}
\Phi(x,\xi) := K(x,\xi)\Sigma^{+-}(\xi) - \int_0^\xi K(x,s)D^+(s,\xi)d\xi\\
- \int_0^1 K(x,s)\Phi(s,\xi)ds.
\end{aligned} \tag{27}$$

This function is well-defined due to the strictly lower triangular structure of K. Explicitly, this can be seen by writing the $(i,j)^{th}$ element out, which reads

$$\begin{aligned}
\phi_{ij}(x,\xi) = \sum_{k=1}^{i-1}\Big(K_{ik}(x,\xi)\sigma^{+-}_{kj}(\xi) - \int_0^\xi K_{ik}(x,s)d^+_{kj}(s,\xi)d\xi\\
- \int_0^1 K_{ik}(x,s)\phi_{kj}(s,\xi)ds\Big).
\end{aligned} \tag{28}$$

Hence, element ϕ_{ij} is defined recursively in terms of the "previously" defined elements $\phi_{1j},\phi_{2j},\dots,\phi_{i-1,j}$ in the same column, starting with $\phi_{1j} = 0$. The target system, with states $\tilde{\gamma} = [\tilde{\gamma}_1,\dots,\tilde{\gamma}_n]^\top$ and $\tilde{\nu} = [\tilde{\nu}_1,\dots,\tilde{\nu}_m]^\top$, is then given by

$$\begin{aligned}
\tilde{\gamma}_t(x,t) + \Lambda^+\tilde{\gamma}_x(x,t) = \Sigma^{+-}(x)\tilde{\nu}(x,t) - \int_x^1 D^+(x,\xi)\tilde{\nu}(\xi,t)d\xi\\
- \int_0^1 \Phi(x,\xi)\tilde{\nu}(\xi,t)d\xi
\end{aligned} \tag{29a}$$

$$\tilde{\nu}_t(x,t) - \Lambda^-\tilde{\nu}_x(x,t) = \Sigma^{--}(x)\tilde{\nu}(x,t) - \int_x^1 D^-(x,\xi)\tilde{\nu}(\xi,t)d\xi \tag{29b}$$

$$\tilde{\gamma}(0,t) = Q_0\tilde{\nu}(0,t) \tag{29c}$$

$$\tilde{\nu}(1,t) = 0 \tag{29d}$$

$$\tilde{\gamma}(x,0) = \tilde{\gamma}_0(x) \tag{29e}$$

$$\tilde{\nu}(x,0) = \tilde{\nu}_0(x). \tag{29f}$$

The initial conditions $\tilde{\gamma}_0 \in L^2((0,1);\mathbb{R}^n)$ and $\tilde{\nu}_0 \in L^2((0,1);\mathbb{R}^m)$.

The proof of the following Lemma relies on similar steps as in the proof of Lemma 11 in [10] together with straightforward application of the method of characteristics, but is included here for completeness.

Lemma 2.4. *The states* $\tilde{\gamma}$ *and* $\tilde{\nu}$*, governed by the error dynamics* (29) *converge to zero in finite time given by* (7)*.*

Proof. By the method of characteristics and cascade structure of (29), we see from (29b) with boundary (29d) that $\tilde{\nu}(x,t) \equiv 0\ \forall t \ge \frac{1}{\mu_1}$. The dynamics (29a) reduces after this to $\tilde{\gamma}_t + \Lambda^+\tilde{\gamma}_x = 0$ with boundary condition $\tilde{\gamma}(0,t) = 0$, which vanishes after an additional time $\frac{1}{\lambda_1}$.

We consider now the Fredholm integral transformation

$$\tilde{\alpha}(x,t) = \tilde{\gamma}(x,t) + \int_0^1 K(x,\xi)\tilde{\gamma}(\xi,t)d\xi \tag{30a}$$

$$\tilde{\beta}(x,t) = \tilde{\nu}(x,t) \tag{30b}$$

with K a solution to (16). We know from Lemma 2 of [25] that since K is strictly lower triangular, the Fredholm integral transformation (30) is invertible.

Lemma 2.5. *The invertible Fredholm integral transformation* (30)*, with K satisfying* (16)*, maps the target error system* (29) *into the intermediate target error system* (22)*.*

Proof. As (30b) is the identity transformation, and the structure of the equation (22b) with boundary (22d) for $\tilde{\beta}$ is identical to the equation (29b) with boundary (29d) for $\tilde{\nu}$, it only remains to prove that $\tilde{\gamma}$ maps into $\tilde{\alpha}$ via (30a).

Differentiating (30a) with respect to time and space, substituting in (29a), integrating by parts and combining with (22a) we find that

$$\begin{aligned}
&\tilde{\alpha}_t(x,t) + \Lambda^+\tilde{\alpha}_x(x,t) - \Sigma^{+-}(x)\tilde{\beta}(x,t) + \int_x^1 D^+(x,\xi)\tilde{\beta}(\xi,t)d\xi \\
&\quad + T^+(x)\tilde{\alpha}(1,t) = \int_0^1 \Bigg(\Phi(x,\xi) - K(x,\xi)\Sigma^{+-}(\xi) \\
&\quad + \int_0^\xi K(x,s)D^+(s,\xi)ds + \int_0^1 K(x,s)\Phi(s,\xi)ds\Bigg)\tilde{\nu}(\xi,t)d\xi \\
&\quad - \int_0^1 \left(K_\xi(x,\xi)\Lambda^+ + \Lambda^+K_x(x,\xi) + T^+(x)K(1,\xi)\right)\tilde{\gamma}(\xi,t)d\xi \\
&\quad + \left(K(x,1)\Lambda^+ - T^+(x)\right)\tilde{\gamma}(1,t) - K(x,0)\Lambda^+(0)Q_0\tilde{\nu}(0,t) = 0.
\end{aligned} \tag{31}$$

From (31) we obtain the definition (27) of Φ, the definition (13) of T^+, the PDE (16a) and boundary condition (16b) at $\xi = 0$. For the second boundary condition (16c), evaluating the Fredholm transform (30) at $x = 0$, substituting into boundary conditions (22c), applying (30a) once more and changing the order of integration gives us

$$\int_0^1 K(0,\xi)\tilde{\gamma}(\xi,t)d\xi = \int_0^1 \left(H(\xi) + \int_0^1 H(s)K(s,\xi)ds\right)\tilde{\gamma}(\xi,t)d\xi \tag{32}$$

from which (16c) trivially follows.

We can now prove Theorem 2.2 by combining Lemmas 2.3–2.5.

Proof (Proof of Theorem 2.2). By Lemma 2.3 and Lemma 2.5, the dynamics of (20) and (29) are equivalent. Since by Lemma 2.4, $(\tilde{\gamma},\tilde{\nu}) = 0$ in finite time given by (7), it follows (see (30) and (21)), that $(\tilde{u},\tilde{v}) = 0$ in finite time given by (7).

3. Minimum time observer with bilateral or in-domain sensing

We consider and solve first the case of bilateral sensing. Subsequently, we show that the case of pointwise in-domain sensing can be derived in similar steps to the case of bilateral sensing, and give conditions for sensor placement to achieve minimum time observer convergence.

3.1. Problem statement

Assume both boundaries of (1) are measured, giving us the measurements $y_0 = [y_{0,1},\dots,y_{0,m}]$, $y_1 = [y_{1,1},\dots,y_{1,n}]$, defined by

$$y_0(t) := v(0,t) \tag{33a}$$

$$y_1(t) := u(1,t). \tag{33b}$$

Given knowledge of the output signals y_0, y_1 and also possible input signals U_0, U_1, we would like to design an observer for (1) that converges in finite time $t_{2,min}$ given by (8). We propose an observer in the form

$$\begin{aligned}
\hat{u}_t(x,t) + \Lambda^+\hat{u}_x(x,t) &= \Sigma^{++}(x)\hat{u}(x,t) + \Sigma^{+-}(x)\hat{v}(x,t) \\
&\quad + P^{++}(x)\left(y_1(t) - \hat{u}(1,t)\right) \\
&\quad + P^{+-}(x)\left(y_0(t) - \hat{v}(0,t)\right) &\text{(34a)}\\
\hat{v}_t(x,t) - \Lambda^-\hat{v}_x(x,t) &= \Sigma^{-+}(x)\hat{u}(x,t) + \Sigma^{--}(x)\hat{v}(x,t) \\
&\quad + P^{-+}(x)\left(y_1(t) - \hat{u}(1,t)\right) \\
&\quad + P^{--}(x)\left(y_0(t) - \hat{v}(0,t)\right) &\text{(34b)}\\
\hat{u}(0,t) &= Q_0y_0(t) + U_0(t) &\text{(34c)}\\
\hat{v}(1,t) &= R_1y_1(t) + U_1(t) &\text{(34d)}\\
\hat{u}(x,0) &= \hat{u}_0(x) &\text{(34e)}\\
\hat{v}(x,0) &= \hat{v}_0(x) &\text{(34f)}
\end{aligned}$$

where P^{++}, P^{+-}, P^{-+} and P^{--} must be chosen to guarantee convergence time $t_{2,min}$. The initial conditions $\hat{u}_0$, $\hat{v}_0$ of the observer (34) are to be established further down.

3.2. Folding the $n+m$ system into an $(n+m)+(n+m)$ system

In this section, we split the spatial domain of the $n+m$ system (1) at an internal point $x_s \in (0,1)$, fold the spatial domain around this point and redefine the states and system parameters accordingly to write the system as a $(n+m)+(n+m)$ system. This allows us subsequently to apply the minimum time unilateral observer design (11)–(16) to the resultant system, giving state estimates in the "folded" coordinates that can then be mapped back to the original coordinates.

Consider the two invertible affine spatial transformations $r_{x_s} : [x_s,1] \mapsto [0,1]$ and $l_{x_s} : [0,x_s] \mapsto [0,1]$, defined by

$$r_{x_s}(x) := \frac{x - x_s}{1 - x_s}, \qquad l_{x_s}(x) := \frac{x_s - x}{x_s} \tag{35}$$

with inverses given by

$$r_{x_s}^{-1}(x) = x_s + x(1 - x_s), \qquad l_{x_s}^{-1}(x) = x_s(1 - x). \tag{36}$$

Next, we define the $(n+m)$-dimensional diagonal matrices denoted $\bar{\Lambda}^+ = \mathrm{diag}\{\bar{\lambda}_1,\dots,\bar{\lambda}_{n+m}\}$, $\bar{\Lambda}^- = \mathrm{diag}\{\bar{\mu}_1,\dots,\bar{\mu}_{n+m}\}$ as

$$\bar{\Lambda}^+ := \Pi^+V^+(\Pi^+)^\top, \qquad \bar{\Lambda}^- := \Pi^-V^-(\Pi^-)^\top, \tag{37}$$

where

$$V^+ := \begin{bmatrix} \frac{1}{1-x_s}\Lambda^+ & 0_{n\times m} \\ 0_{m\times n} & \frac{1}{x_s}\Lambda^- \end{bmatrix}, \quad V^- := \begin{bmatrix} \frac{1}{x_s}\Lambda^+ & 0_{n\times m} \\ 0_{m\times n} & \frac{1}{1-x_s}\Lambda^- \end{bmatrix}, \tag{38}$$

and Π^+, Π^- are any $(n+m)\times(n+m)$ permutation matrices defined such that

$$-\bar{\mu}_{n+m} \leq \cdots \leq -\bar{\mu}_1 < 0 < \bar{\lambda}_1 \leq \cdots \leq \bar{\lambda}_{n+m} \tag{39}$$

is true. Furthermore, define $(n+m)\times(n+m)$ matrix valued functions $\bar{\Sigma}^{++}$, $\bar{\Sigma}^{+-}$, $\bar{\Sigma}^{-+}$ and $\bar{\Sigma}^{--}$ as

$$\bar{\Sigma}^{++}(x) := \Pi^+\Xi^{++}(x)(\Pi^+)^\top, \quad \bar{\Sigma}^{+-}(x) := \Pi^+\Xi^{+-}(x)(\Pi^-)^\top \tag{40a}$$

$$\bar{\Sigma}^{-+}(x) := \Pi^-\Xi^{-+}(x)(\Pi^+)^\top, \quad \bar{\Sigma}^{--}(x) := \Pi^-\Xi^{--}(x)(\Pi^-)^\top \tag{40b}$$

where

$$\Xi^{++}(x) := \begin{bmatrix} \Sigma^{++}(r_{x_s}^{-1}(x)) & 0_{n\times m} \\ 0_{m\times n} & \Sigma^{--}(l_{x_s}^{-1}(x)) \end{bmatrix}, \tag{41a}$$

$$\Xi^{+-}(x) := \begin{bmatrix} 0_{n\times n} & \Sigma^{+-}(r_{x_s}^{-1}(x)) \\ \Sigma^{-+}(l_{x_s}^{-1}(x)) & 0_{m\times m} \end{bmatrix}, \tag{41b}$$

$$\Xi^{-+}(x) := \begin{bmatrix} 0_{n\times n} & \Sigma^{+-}(l_{x_s}^{-1}(x)) \\ \Sigma^{-+}(r_{x_s}^{-1}(x)) & 0_{m\times m} \end{bmatrix}, \tag{41c}$$

$$\Xi^{--}(x) := \begin{bmatrix} \Sigma^{++}(l_{x_s}^{-1}(x)) & 0_{n\times m} \\ 0_{m\times n} & \Sigma^{--}(r_{x_s}^{-1}(x)) \end{bmatrix}. \tag{41d}$$

Lastly, denote the boundary reflection matrices by

$$\bar{Q}_0 := \Pi^+(\Pi^-)^\top, \qquad \bar{R}_1 := \Pi^-\Gamma(\Pi^+)^\top \tag{42}$$

with

$$\Gamma := \begin{bmatrix} 0_{n\times n} & Q_0 \\ R_1 & 0_{m\times m} \end{bmatrix}. \tag{43}$$

With these quantities defined, we can state the following Lemma.

Lemma 3.1. *Let the transformation* $T : (L_2([0,1]))^{n+m} \mapsto (L_2([0,1]))^{2n+2m}$ *be defined by*

$$T[u,v](x) = \left(\Pi^+\begin{bmatrix} u(r_{x_s}^{-1}(x)) \\ v(l_{x_s}^{-1}(x)) \end{bmatrix}, \Pi^-\begin{bmatrix} u(l_{x_s}^{-1}(x)) \\ v(r_{x_s}^{-1}(x)) \end{bmatrix}\right) \tag{44}$$

with inverse $T^{-1} : (L_2([0,1]))^{2n+2m} \mapsto (L_2([0,1]))^{n+m}$ *given by*[2]

$$T^{-1}[\bar{u},\bar{v}] = \begin{cases} \left(((\Pi^-)^\top\bar{v})_{[1:n]}(l_{x_s}(x)), ((\Pi^+)^\top\bar{u})_{[(n+1):(n+m)]}(l_{x_s}(x))\right), \\ \qquad\qquad \text{if } 0 \leq x < x_s \\ \left(((\Pi^+)^\top\bar{u})_{[1:n]}(r_{x_s}(x)), ((\Pi^-)^\top\bar{v})_{[(n+1):(n+m)]}(r_{x_s}(x))\right), \\ \qquad\qquad \text{if } x_s \leq x \leq 1 \end{cases} \tag{45}$$

[2]Given an $n\times m$ matrix A, by the notation $A_{[i:j,k:l]}$, with $1 \leq i \leq j \leq n$, $1 \leq k \leq l \leq m$, we denote the $(j-i+1)\times(l-k+1)$ sub-matrix consisting of all elements between and including row number i and j, column number k and l.

The invertible change of coordinates $(\bar{u}(x,t),\bar{v}(x,t)) = T[u,v](x,t)$ *maps* (1) *into*

$$\bar{u}_t(x,t) + \bar{\Lambda}^+\bar{u}_x(x,t) = \bar{\Sigma}^{++}\bar{u}(x,t) + \bar{\Sigma}^{+-}\bar{v}(x,t) \tag{46a}$$

$$\bar{v}_t(x,t) - \bar{\Lambda}^-\bar{v}_x(x,t) = \bar{\Sigma}^{+-}\bar{u}(x,t) + \bar{\Sigma}^{--}\bar{v}(x,t) \tag{46b}$$

$$\bar{u}(0,t) = \bar{Q}_0\bar{v}(0,t) \tag{46c}$$

$$\bar{v}(1,t) = \bar{R}_1\bar{u}(1,t) + \bar{U}(t) \tag{46d}$$

$$\bar{u}(x,0) = \bar{u}_0(x) \tag{46e}$$

$$\bar{v}(x,0) = \bar{v}_0(x), \tag{46f}$$

with coefficients given by (37)–(43) *and boundary input*

$$\bar{U} := \Pi^-\begin{bmatrix} U_0 \\ U_1 \end{bmatrix}. \tag{47}$$

Proof. Differentiating (44) with respect to x and applying the chain rule we can express $\bar{u}_x$ and $\bar{v}_x$ in terms of u_x and v_x as

$$\begin{aligned} \bar{u}_x(x,t) &= \Pi^+\begin{bmatrix} (1-x_s)u_x(r_{x_s}^{-1}(x),t) \\ -x_s v_x(l_{x_s}^{-1}(x),t) \end{bmatrix}, \\ \bar{v}_x(x,t) &= \Pi^-\begin{bmatrix} -x_s u_x(l_{x_s}^{-1}(x),t) \\ (1-x_s)v_x(r_{x_s}^{-1}(x),t) \end{bmatrix}. \end{aligned} \tag{48}$$

Also, differentiating (44) with respect to time, we find

$$\bar{u}_t(x,t) = \Pi^+\begin{bmatrix} u_t(r_{x_s}^{-1}(x),t) \\ v_t(l_{x_s}^{-1}(x),t) \end{bmatrix}, \quad \bar{v}_t(x,t) = \Pi^-\begin{bmatrix} u_t(l_{x_s}^{-1}(x),t) \\ v_t(r_{x_s}^{-1}(x),t) \end{bmatrix}. \tag{49}$$

Inserting (48) and (49) into (46) and comparing to (1) we find the transport speeds can be assigned as (37)–(38) and the coupling coefficients become (40)–(41). Applying (44) for $x = 0$ and $x = 1$ we find

$$\bar{u}(0,t) = \Pi^+\begin{bmatrix} u(x_s,t) \\ v(x_s,t) \end{bmatrix}, \qquad \bar{v}(0,t) = \Pi^-\begin{bmatrix} u(x_s,t) \\ v(x_s,t) \end{bmatrix} \tag{50a}$$

$$\bar{u}(1,t) = \Pi^+\begin{bmatrix} u(1,t) \\ v(0,t) \end{bmatrix}, \qquad \bar{v}(1,t) = \Pi^-\begin{bmatrix} u(0,t) \\ v(1,t) \end{bmatrix} \tag{50b}$$

which confirms that the boundary condition matrices are given by (42) along with the input signal assignments given by (47).

Remark 3.2. *Note that for the boundary condition* (46c) *to be well-defined and to subsequently conclude a unique (weak) solution of* (46)*, within the scope of this section we firstly let the initial conditions in* (46e)–(46f) *satisfy* $\bar{u}_0, \bar{v}_0 \in L^2((0,1);\mathbb{R}^{n+m})$*, and subsequently the initial conditions in* (1e)–(1e) *are defined in terms of these as*

$$\begin{bmatrix} u_0(x) \\ v_0(x) \end{bmatrix} = T^{-1}[\bar{u}_0,\bar{v}_0](x). \tag{51}$$

The regularity of solutions for systems in this section is hence determined from the regularity of solutions of (46) *and associated observer and error system. As for* (1) *in Section 1, it can be shown that for* (46) *there is a unique (weak) solution* $\bar{u},\bar{v} \in C^0([0,\infty);L^2((0,1);\mathbb{R}^{n+m}))$.

3.3. Minimum time bilateral observer

With the $(n+m)+(n+m)$ system (46) defined, by noting that the vector of known output signals defined as

$$\bar{y}(t) := \Pi^{+}\begin{bmatrix} y_1(t) \\ y_0(t) \end{bmatrix} \tag{52}$$

can also be expressed as $\bar{y} = \bar{u}(1)$, Theorem 2.2 is applied to make a unilateral observer for (46), producing estimates $(\check{u}, \check{v})$ that converge to $(\bar{u}, \bar{v})$ in finite time

$$\bar{t}_{1,min} = \frac{1}{\bar{\lambda}_1} + \frac{1}{\bar{\mu}_1}. \tag{53}$$

This observer is expressed as

$$\begin{aligned}
\check{u}_t(x,t) + \bar{\Lambda}^{+}\check{u}_x(x,t) &= \bar{\Sigma}^{++}(x)\check{u}(x,t) + \bar{\Sigma}^{+-}(x)\check{v}(x,t) \\
&\quad + \bar{P}^{+}(x)(\bar{y}(t) - \check{u}(1,t)) && \text{(54a)} \\
\check{v}_t(x,t) - \bar{\Lambda}^{-}\check{v}_x(x,t) &= \bar{\Sigma}^{-+}(x)\check{u}(x,t) + \bar{\Sigma}^{--}(x)\check{v}(x,t) \\
&\quad + \bar{P}^{-}(x)(\bar{y}(t) - \check{u}(1,t)) && \text{(54b)} \\
\check{u}(0,t) &= \bar{Q}_0\check{v}(0,t) && \text{(54c)} \\
\check{v}(1,t) &= \bar{R}_1\bar{y}(t) + \bar{U}(t) && \text{(54d)} \\
\check{u}(x,0) &= \check{u}_0(x) && \text{(54e)} \\
\check{v}(x,t) &= \check{v}_0(x) && \text{(54f)}
\end{aligned}$$

with the observer gains $\bar{P}^{+}$, $\bar{P}^{-}$ being $(n+m)\times(n+m)$ matrix-valued functions computed according to the expressions (12), but using $(n+m)\times(n+m)$ matrix valued functions $\bar{M}$, $\bar{N}$ that are solutions to equations (14) solved using system coefficients of (46). Also, $\bar{K}$ is a $(n+m)\times(n+m)$ strictly lower triangular matrix valued function solved from the equation (16), also with coefficients from (46). The observer (54) is initialized by $\check{u}_0, \check{v}_0 \in L^2((0,1);\mathbb{R}^{n+m})$, and recognizing that (54) is a specific realization of (11) we conclude that (54) has a unique (weak) solution $\check{u}, \check{v} \in C^0([0,\infty); L^2((0,1);\mathbb{R}^{n+m}))$. Based on $\check{u}_0, \check{v}_0$, we set the initial conditions of the bilateral observer (34) as

$$\begin{bmatrix} \hat{u}_0(x) \\ \hat{v}_0(x) \end{bmatrix} = T^{-1}[\check{u}_0, \check{v}_0](x). \tag{55}$$

Remark 3.3. *Note that as long as the assumption* (4) *on the transport speeds of the original system* (1) *holds, imposing the seemingly weaker conditions* (39) *on the transformed system* (46) *is sufficient for $\bar{M}$, $\bar{N}$ to have a well-posed solution. This can be seen by pre- and post-multiplying* (14c) *by respectively Π^{+} and $(\Pi^{+})^{\top}$, and verifying that the resultant boundary conditions are well-defined. Writing* (14f) *in matrix form, the same argument can be applied.*

Let the $(n+m)\times(n+m)$ matrix valued functions $\underline{P}^{+}, \underline{P}^{-}$ be defined in terms of $\bar{P}^{+}$, $\bar{P}^{-}$ used in (54) as

$$\underline{P}^{+}(x) := (\Pi^{+})^{\top}\bar{P}^{+}(x)\Pi^{+} \qquad \underline{P}^{-}(x) := (\Pi^{-})^{\top}\bar{P}^{-}(x)\Pi^{+}. \tag{56}$$

We are now in a position to define the observer gains P^{++}, P^{+-}, P^{-+} and P^{--} appearing in the observer (34).

Lemma 3.4. *The invertible change of coordinates $(\hat{u}(x,t), \hat{v}(x,t)) = T^{-1}[\check{u}, \check{v}](x,t)$, defined as* (45)*, maps* (54) *into* (34)*, with observer gains given in terms of* (56) *as*

$$P^{++}(x) := \begin{cases} \underline{P}^{-}_{[1:n,\ 1:n]}(l_{x_s}(x)), & \text{if } 0 \le x < x_s \\ \underline{P}^{+}_{[1:n,\ 1:n]}(r_{x_s}(x)), & \text{if } x_s \le x \le 1 \end{cases} \tag{57a}$$

$$P^{+-}(x) := \begin{cases} \underline{P}^{-}_{[1:n,\ (n+1):(n+m)]}(l_{x_s}(x)), & \text{if } 0 \le x < x_s \\ \underline{P}^{+}_{[1:n,\ (n+1):(n+m)]}(r_{x_s}(x)), & \text{if } x_s \le x \le 1 \end{cases} \tag{57b}$$

$$P^{-+}(x) := \begin{cases} \underline{P}^{+}_{[(n+1):(n+m),\ 1:n]}(l_{x_s}(x)), & \text{if } 0 \le x < x_s \\ \underline{P}^{-}_{[(n+1):(n+m),\ 1:n]}(r_{x_s}(x)), & \text{if } x_s \le x \le 1 \end{cases} \tag{57c}$$

$$P^{--}(x) := \begin{cases} \underline{P}^{+}_{[(n+1):(n+m),\ (n+1):(n+m)]}(l_{x_s}(x)), & \text{if } 0 \le x < x_s \\ \underline{P}^{-}_{[(n+1):(n+m),\ (n+1):(n+m)]}(r_{x_s}(x)), & \text{if } x_s \le x \le 1 \end{cases} \tag{57d}$$

Proof. Start by premultiplying (54a) by $(\Pi^{+})^{\top}$ to obtain

$$\begin{aligned}
&(\Pi^{+})^{\top}\check{u}_t(x,t) + \underbrace{(\Pi^{+})^{\top}\bar{\Lambda}^{+}\Pi^{+}}_{V^{+}}(\Pi^{+})^{\top}\check{u}_x(x,t) \\
&= \underbrace{(\Pi^{+})^{\top}\bar{\Sigma}^{++}(x)\Pi^{+}}_{\Xi^{++}(x)}(\Pi^{+})^{\top}\check{u}(x,t) + \underbrace{(\Pi^{+})^{\top}\bar{\Sigma}^{+-}(x)\Pi^{-}}_{\Xi^{+-}(x)}(\Pi^{-})^{\top}\check{v}(x,t) \\
&\quad + \underbrace{(\Pi^{+})^{\top}\bar{P}^{+}(x)\Pi^{+}}_{\underline{P}^{+}(x)}\Big((\Pi^{+})^{\top}\bar{y}(t) - (\Pi^{+})^{\top}\check{u}(1,t)\Big).
\end{aligned} \tag{58}$$

Likewise, premultiplying (54b) with $(\Pi^{-})^{\top}$ yields

$$\begin{aligned}
&(\Pi^{-})^{\top}\check{v}_t(x,t) - V^{-}(\Pi^{-})^{\top}\check{v}_x(x,t) \\
&= \Xi^{-+}(x)(\Pi^{+})^{\top}\check{u}(x,t) + \Xi^{--}(x)(\Pi^{-})^{\top}\check{v}(x,t) \\
&\quad + \underline{P}^{-}(x)\Big((\Pi^{+})^{\top}\bar{y}(t) - (\Pi^{+})^{\top}\check{u}(1,t)\Big).
\end{aligned} \tag{59}$$

Consider now the dynamics (58)–(59) of respectively $(\Pi^{+})^{\top}\check{u}$, $(\Pi^{-})^{\top}\check{v}$, over the left sub-interval $x \in [0, x_s]$. From (45) we have $\hat{u}(x,t) = ((\Pi^{-})^{\top}\check{v})_{[1:n]}(l_{x_s}(x),t)$ and $\hat{v}(x,t) = ((\Pi^{+})^{\top}\check{u})_{[(n+1):(n+m)]}(l_{x_s}(x),t)$. Taking the first n equations from (59), and the last m equations from (58), applying the coefficient assignments (38),(41), and substituting in $\hat{u}(x,t)$ and $\hat{v}(x,t)$ along their respective partial derivatives, which are equivalent to the ones from (48)–(49) premultiplied by $(\Pi^{+})^{\top}$, $(\Pi^{-})^{\top}$, respectively for $\check{u}$, $\check{v}$, we find

$$\begin{aligned}
\hat{u}_t(x,t) - \frac{1}{x_s}\Lambda^{+}(-x_s\hat{u}_x(x,t)) &= \Sigma^{+-}(x)\hat{v}(x,t) + \Sigma^{++}(x)\hat{u}(x,t) \\
&\quad + \underline{P}^{-}_{[1:n,1:n]}(l_{x_s}(x))(y_1(t) - \hat{u}(1,t)) \\
&\quad + \underline{P}^{-}_{[1:n,(n+1):(n+m)]}(l_{x_s}(x))(y_0(t) - \hat{v}(0,t)) && \text{(60a)} \\
\hat{v}(x,t) + \frac{1}{x_s}\Lambda^{-}(-x_s\hat{v}_x(x,t)) &= \Sigma^{--}(x)\hat{v}(x,t) + \Sigma^{-+}(x)\hat{u}(x,t) \\
&\quad + \underline{P}^{+}_{[(n+1):(n+m),1:n]}(l_{x_s}(x))(y_1(t) - \hat{u}(1,t)) \\
&\quad + \underline{P}^{+}_{[(n+1):(n+m),(n+1):(n+m)]}(l_{x_s}(x))(y_0(t) - \hat{v}(0,t)). && \text{(60b)}
\end{aligned}$$

Comparing (60) to (34), we obtain the observer gains in (57) valid for all $x \in [0, x_s]$. Applying the same steps for the right sub-interval $x \in (x_s, 1]$, the observer gain assignments in (57) valid for all $x \in (x_s, 1]$ are obtained.

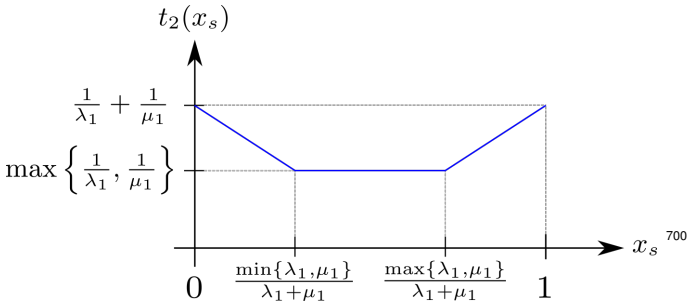

Figure 4: Convergence time t_2 of bilateral observer as a function of splitting point x_s.

Theorem 3.5. *Consider system* (1) *with outputs* (33) *and the observer* (34). *If the output injection gains are selected as* (57) *with x_s satisfying*

$$\frac{\min\{\lambda_1,\mu_1\}}{\mu_1+\lambda_1} \leq x_s \leq \frac{\max\{\lambda_1,\mu_1\}}{\mu_1+\lambda_1}, \tag{61}$$

then for all times $t \geq t_{2,min}$, we have that $(\hat{u}(\cdot,t),\hat{v}(\cdot,t)) = (u(\cdot,t),v(\cdot,t))$.

Proof. From Lemma 3.4 we know that (34) is mapped into (54) using the invertible transform (44). Next, from Theorem 2.2 we know that (54) produces state estimates $(\check{u},\check{v})$ that converge to the states $(\bar{u},\bar{v})$ of (46) in finite time $\bar{t}_{1,min}$ given by (53). Due to the equivalence of (46) and (1) by Lemma 3.1 via the transformation T in (44), and the corresponding inverse T^{-1} in (45), choosing bilateral gains as (57) allows us to conclude that the estimates $(\hat{u},\hat{v})$ produced by (34) converge to the states (u,v) of (1), in finite time $t_2 = \bar{t}_{1,min}$.

Expressing this convergence time as a function of x_s and equating the transport speeds of (46) with the transport speeds of (1), via (37)–(38), we have

$$\begin{aligned} t_2(x_s) &= \frac{1}{\bar{\lambda}_1(x_s)} + \frac{1}{\bar{\mu}_1(x_s)} \\ &= \max\left\{\frac{1-x_s}{\lambda_1},\frac{x_s}{\mu_1}\right\} + \max\left\{\frac{x_s}{\lambda_1},\frac{1-x_s}{\mu_1}\right\}. \end{aligned} \tag{62}$$

In both terms a strictly increasing and decreasing linear function is being compared, and hence we can identify that convergence speeds for different values of x_s are given by

$$t_2(x_s) = \begin{cases} \frac{1-x_s}{\lambda_1}+\frac{1-x_s}{\mu_1}, & \text{if } 0 < x_s < \frac{\min\{\lambda_1,\mu_1\}}{\mu_1+\lambda_1} \\ \max\{\frac{1}{\lambda_1},\frac{1}{\mu_1}\}, & \text{if } \frac{\min\{\lambda_1,\mu_1\}}{\mu_1+\lambda_1} \leq x_s \leq \frac{\max\{\lambda_1,\mu_1\}}{\mu_1+\lambda_1} \\ \frac{x_s}{\lambda_1}+\frac{x_s}{\mu_1}, & \text{if } \frac{\max\{\lambda_1,\mu_1\}}{\mu_1+\lambda_1} < x_s < 1 \end{cases} \tag{63}$$

from which we identify the interval (61) that x_s must be contained in to achieve convergence within time $t_{2,min}$. Figure 4 shows the general shape of the function in (63).

3.4. Minimum time observer for pointwise in-domain sensing

We consider now the third case of sensor placement, namely that sensing of (1) is performed at a single in-domain point $x_s \in (0,1)$. In other words, it is assumed that the signal vector

$$y_s(t) = \begin{bmatrix} u(x_s,t) \\ v(x_s,t) \end{bmatrix} \tag{64}$$

is known, only. Using this, we aim to design observer gains P_s^+, P_s^-, so that the observer

$$\begin{aligned} \hat{u}_t(x,t) + \Lambda^+\hat{u}_x(x,t) &= \Sigma^{++}(x)\hat{u}(x,t) + \Sigma^{+-}(x)\hat{v}(x,t) \\ &\quad + P_s^+(x)\left(y_s(t) - \begin{bmatrix}\hat{u}(x_s,t)\\ \hat{v}(x_s,t)\end{bmatrix}\right) \end{aligned} \tag{65a}$$

$$\begin{aligned} \hat{v}_t(x,t) - \Lambda^-\hat{v}_x(x,t) &= \Sigma^{-+}(x)\hat{u}(x,t) + \Sigma^{--}(x)\hat{v}(x,t) \\ &\quad + P_s^-(x)\left(y_s(t) - \begin{bmatrix}\hat{u}(x_s,t)\\ \hat{v}(x_s,t)\end{bmatrix}\right) \end{aligned} \tag{65b}$$

$$\hat{u}(0,t) = Q_0\hat{v}(0,t) + U_0(t) \tag{65c}$$

$$\hat{v}(1,t) = R_1\hat{u}(1,t) + U_1(t) \tag{65d}$$

$$\hat{u}(x,0) = \hat{u}_0(x) \tag{65e}$$

$$\hat{v}(x,0) = \hat{v}_0(x) \tag{65f}$$

converges in minimum time $t_{2,min}$ given by (8). The initial conditions of the observer (65) are assigned in terms of the initial conditions $\check{u}_0,\check{v}_0$ of (54) as

$$\begin{bmatrix}\hat{u}_0\\ \hat{v}_0\end{bmatrix} = T^{-1}[\check{u}_0,\check{v}_0](1-x). \tag{66}$$

Using the gains $\bar{P}^+$, $\bar{P}^-$ appearing in (54), let the $(n+m)\times(n+m)$ matrix-valued functions L^+, L^- be defined in terms of these as

$$L^+(x) := (\Pi^+)^\top\bar{P}^-(1-x)\Pi^-, \quad L^-(x) := (\Pi^-)^\top\bar{P}^+(1-x)\Pi^-. \tag{67}$$

We are now in a position to state the following Corollary specifying the necessary observer gains and conditions on sensor placement for minimum time convergence to be achieved.

Corollary 3.6. *Consider the system* (1) *with measurement* (64) *and observer* (65). *If the measurement y_s is taken at a point x_s that satisfies inequality* (61), *then choosing the observer gains as*

$$P_s^+(x) = \begin{cases} L^-_{[1:n,1:(n+m)]}(l_{x_s}(x)), & \text{if } 0 \leq x \leq x_s \\ L^+_{[1:n,1:(n+m)]}(r_{x_s}(x)), & \text{if } x_s < x \leq 1 \end{cases} \tag{68a}$$

$$P_s^-(x) = \begin{cases} L^+_{[(n+1):(n+m),1:(n+m)]}(l_{x_s}(x)), & \text{if } 0 \leq x \leq x_s \\ L^-_{[(n+1):(n+m),1:(n+m)]}(r_{x_s}(x)), & \text{if } x_s < x \leq 1 \end{cases} \tag{68b}$$

guarantees that for all times $t \geq t_{2,min}$, we have $(\hat{u}(\cdot,t),\hat{v}(\cdot,t)) = (u(\cdot,t),v(\cdot,t))$.

Proof. As shown by Lemma 3.1, choosing the folding point as x_s, system (1) can be mapped into system (46) via the mapping T in (44). Consider an observer for the resultant system given by

$$\begin{aligned} \check{u}_t(x,t) + \bar{\Lambda}^+(x)\check{u}_x(x,t) &= \bar{\Sigma}^{++}(x)\check{u}(x,t) + \bar{\Sigma}^{+-}(x)\check{v}(x,t) \\ &\quad + \bar{L}^+(x)(\bar{y}_0(t) - \check{v}(0,t)) \end{aligned} \tag{69a}$$

$$\begin{aligned} \check{v}_t(x,t) - \bar{\Lambda}^-(x)\check{v}_x(x,t) &= \bar{\Sigma}^{-+}(x)\check{u}(x,t) + \bar{\Sigma}^{--}(x)\check{v}(x,t) \\ &\quad + \bar{L}^-(x)(\bar{y}_0(t) - \check{v}(0,t)) \end{aligned} \tag{69b}$$

$$\check{u}(0,t) = \bar{Q}_0\bar{y}_0(t) \tag{69c}$$

$$\check{v}(1,t) = \bar{R}_1\check{u}(1,t) + \bar{U}(t) \tag{69d}$$
$$\check{u}(x,0) = \check{u}_0(x) \tag{69e}$$
$$\check{v}(x,0) = \check{v}_0(x) \tag{69f}$$

which differs from (54) in that the measurement $\bar{y}_0 = \bar{v}(0)$ is known instead of $\bar{y}_1 = \bar{u}(1)$. By symmetry, we see that the observer gains of (69) can be defined in terms of the ones from (54) as

$$\bar{L}^+(x) := \bar{P}^-(1-x), \qquad \bar{L}^-(x) := \bar{P}^+(1-x). \tag{70}$$

Next, by applying the inverse transformation T^{-1} from (45) to (69) and following the same steps as in the Proof of Lemma 3.4, we obtain the gains (68) defined in terms of (67). Finally, applying the same reasoning as in the Proof of Theorem 3.5, we see the observer (65) converges in time $t_{2,min}$ given by (8), provided that x_s satisfies (61).

4. Simulations

In this section a simulation example is presented. A system of the form (1) with $n = 2$, $m = 1$ is implemented in `MATLAB`, along with three observers with different convergence times:

1. The non-minimum time observer from [10] using measurement $y = u(1,\cdot)$.
2. The minimum time observer (11)–(12) using measurement $y = u(1,\cdot)$.
3. The minimum time observer (34),(57) using both measurement $y_0 = v(0,\cdot)$ and $y_1 = u(1,\cdot)$.

4.1. Simulation example

4.1.1. System coefficients

The system (1) for $n = 2$, $m = 1$ is implemented with the coefficients

$$\lambda_1 = \frac{1}{3}, \qquad \lambda_2 = \frac{1}{2}, \qquad \mu_1 = 1,$$
$$\sigma_{12}^{++}(x) = -\frac{\sqrt{x}}{5}, \quad \sigma_{21}^{++}(x) = \frac{3}{50}, \quad \sigma_{11}^{+-}(x) = -\frac{\cos(x)}{50},$$
$$\sigma_{21}^{+-}(x) = -\frac{1}{25}, \quad \sigma_{11}^{-+}(x) = \frac{1}{10}e^{-x}, \quad \sigma_{12}^{-+}(x) = \frac{x}{5},$$
$$\rho_{11} = \frac{1}{5}, \qquad \rho_{12} = \frac{3}{10}, \qquad q_{11} = \frac{1}{2},$$
$$q_{21} = 1.$$

together with inputs and initial conditions

$$U_{11}(t) = -\cos\left(\frac{t}{10}\right), \quad U_{01}(t) = \sqrt{t}, \quad U_{02}(t) = \sin(t),$$
$$u_{1,0}(x) = 1, \qquad u_{2,0}(x) = x, \qquad v_{1,0}(x) = x^2.$$

The input signals are chosen to excite the system, and together with the choice of coefficients and initial conditions the system does not converge to zero but stays marginally stable.

As stated above, three different observers with strictly different convergence times are implemented. For the chosen system coefficients, these three convergence times are respectively

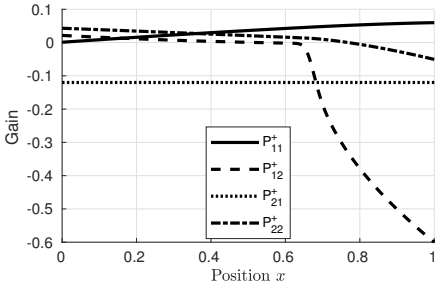

(a) Components P_{11}^+, P_{12}^+, P_{21}^+ and P_{22}^+.

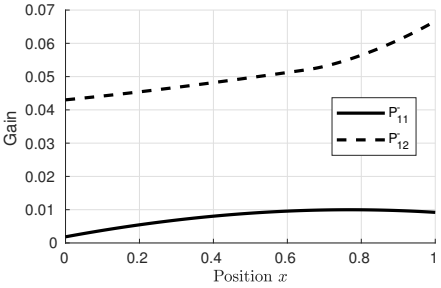

(b) Components P_{11}^- and P_{12}^-.

Figure 5: Non-minimum time observer gains P^+, P^-.

1. $t_{1,nonmin} = \frac{1}{\lambda_1} + \frac{1}{\lambda_2} + \frac{1}{\mu_1} = 6$
2. $t_{1,min} = \frac{1}{\lambda_1} + \frac{1}{\mu_1} = 4$
3. $t_{2,min} = \frac{1}{\lambda_1} = 3.$

Next, observer gains to achieve these convergence times are computed based on the theory presented in Sections 2–3, and in the subsequent section results from a comparative simulation are given. The observer gains are found based on kernels computed by applying the *Uniformly Gridded Discretization* method described Appendix F of [29]. The specific kernel equations that are solved are written out in Appendix A.

4.1.2. Non-minimum time gains

The non-minimum time observer from [10] has the form (11), but instead of gains given by (12), the gains are

$$P^+(x) = M(x,1)\Lambda^+, \qquad P^-(x) = N(x,1)\Lambda^+. \tag{71}$$

These require computation of the kernels (14)–(15) with coefficients defined in section 4.1. Using the resultant numerical solutions of the kernels, the non-minimum time observer gains are assigned as

$$\begin{bmatrix} P_{11}^+(x) & P_{12}^+(x) \\ P_{21}^+(x) & P_{22}^+(x) \end{bmatrix} = \begin{bmatrix} \lambda_1 M_{11}(x,1) & \lambda_2 M_{12}(x,1) \\ \lambda_1 M_{21}(x,1) & \lambda_2 M_{22}(x,1) \end{bmatrix} \tag{72a}$$
$$\begin{bmatrix} P_{11}^-(x) & P_{12}^-(x) \end{bmatrix} = \begin{bmatrix} \lambda_1 N_{11}(x,1) & \lambda_2 N_{12}(x,1) \end{bmatrix} \tag{72b}$$

and are shown in Figure 5.

4.1.3. Minimum time unilateral gains

As stated by Theorem 2.2, to achieve minimum time convergence (7) for unilateral sensing, slightly more complicated

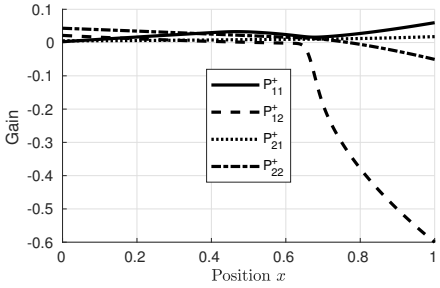

(a) Components P^+_{11}, P^+_{12}, P^+_{21} and P^+_{22}.

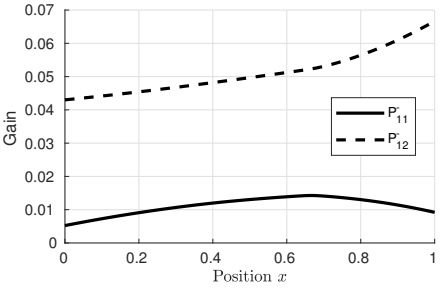

(b) Components P^-_{11} and P^-_{12}.

Figure 6: Minimum time observer gains P^+, P^-.

observer gains must be solved. Calculating these requires the computation of the additional kernel equation (16). The minimum time observer gains are then expressed as

$$\begin{aligned}\begin{bmatrix} P^+_{11}(x) & P^+_{12}(x) \\ P^+_{21}(x) & P^+_{22}(x)\end{bmatrix} &= \begin{bmatrix} \lambda_1 M_{11}(x,1) & \lambda_2 M_{12}(x,1) \\ \lambda_1 M_{21}(x,1) & \lambda_2 M_{22}(x,1)\end{bmatrix} \\ &\quad + \begin{bmatrix} 0 & 0 \\ \lambda_1 k_{21}(x,1) & 0\end{bmatrix} \\ &\quad + \int_x^1 \begin{bmatrix} \lambda_1 M_{12}(x,\xi) k_{21}(\xi,1) & 0 \\ \lambda_1 M_{22}(x,\xi) k_{21}(\xi,1) & 0\end{bmatrix} d\xi \end{aligned} \tag{73a}$$

$$\begin{aligned}\begin{bmatrix} P^-_{11}(x) & P^-_{12}(x)\end{bmatrix} &= \begin{bmatrix} \lambda_1 N_{11}(x,1) & \lambda_2 N_{12}(x,1)\end{bmatrix} \\ &\quad + \int_x^1 \begin{bmatrix} \lambda_1 N_{12}(x,\xi) k_{21}(\xi,1) & 0\end{bmatrix} d\xi \end{aligned} \tag{73b}$$

which are shown in Figure 6.

4.1.4. Minimum time bilateral gains

When both boundaries are measured, Theorem 3.5 guarantees a lower minimum time convergence (8) if x_s is chosen to satisfy (61), which in this example is $\frac{1}{4} \le x_s \le \frac{3}{4}$. For simplicity, choose $x_s = \frac{1}{2}$. This results in observer gains assigned as

$$\begin{bmatrix} P^{++}_{11}(x) & P^{++}_{12}(x) \\ P^{++}_{21}(x) & P^{++}_{22}(x)\end{bmatrix} = \begin{cases} \begin{bmatrix} \underline{P}^-_{11}(1-2x) & \underline{P}^-_{12}(1-2x) \\ \underline{P}^-_{21}(1-2x) & \underline{P}^-_{22}(1-2x)\end{bmatrix}, \\ \qquad\qquad \text{if } 0 \le x \le \frac{1}{2} \\ \begin{bmatrix} \underline{P}^+_{11}(2x-1) & \underline{P}^+_{12}(2x-1) \\ \underline{P}^+_{21}(2x-1) & \underline{P}^+_{22}(2x-1)\end{bmatrix}, \\ \qquad\qquad \text{if } \frac{1}{2} < x \le 1 \end{cases} \tag{74a}$$

$$\begin{bmatrix} P^{+-}_{11}(x) \\ P^{+-}_{21}(x)\end{bmatrix} = \begin{cases} \begin{bmatrix} \underline{P}^-_{13}(1-2x) \\ \underline{P}^-_{23}(1-2x)\end{bmatrix}, \text{ if } 0 \le x \le \frac{1}{2} \\ \begin{bmatrix} \underline{P}^+_{13}(2x-1) \\ \underline{P}^+_{23}(2x-1)\end{bmatrix}, \text{ if } \frac{1}{2} < x \le 1 \end{cases} \tag{74b}$$

$$\begin{bmatrix} P^{-+}_{11}(x) & P^{-+}_{12}(x)\end{bmatrix} = \begin{cases} \begin{bmatrix} \underline{P}^+_{31}(1-2x) & \underline{P}^+_{32}(1-2x)\end{bmatrix}, \\ \qquad\qquad \text{if } 0 \le x \le \frac{1}{2} \\ \begin{bmatrix} \underline{P}^-_{31}(2x-1) & \underline{P}^-_{32}(2x-1)\end{bmatrix}, \\ \qquad\qquad \text{if } \frac{1}{2} < x \le 1 \end{cases} \tag{74c}$$

$$P^{--}_{11}(x) = \begin{cases} \underline{P}^+_{33}(1-2x), \text{ if } 0 \le x \le \frac{1}{2} \\ \underline{P}^-_{33}(2x-1), \text{ if } \frac{1}{2} < x \le 1 \end{cases} \tag{74d}$$

where the elements of $\underline{P}^+$, $\underline{P}^-$ are assigned according to[3] (57) as

$$\begin{aligned}&\begin{bmatrix} \underline{P}^+_{11}(x) & \underline{P}^+_{12}(x) & \underline{P}^+_{13}(x) \\ \underline{P}^+_{21}(x) & \underline{P}^+_{22}(x) & \underline{P}^+_{23}(x) \\ \underline{P}^+_{31}(x) & \underline{P}^+_{32}(x) & \underline{P}^+_{33}(x)\end{bmatrix} = \\ &\quad \begin{bmatrix} 2\lambda_1 \bar{M}_{11}(x,1) & 2\lambda_2 \bar{M}_{12}(x,1) & 2\mu_1 \bar{M}_{13}(x,1) \\ 2\lambda_1 \bar{M}_{21}(x,1) & 2\lambda_2 \bar{M}_{22}(x,1) & 2\mu_1 \bar{M}_{23}(x,1) \\ 2\lambda_1 \bar{M}_{31}(x,1) & 2\lambda_2 \bar{M}_{32}(x,1) & 2\mu_1 \bar{M}_{33}(x,1)\end{bmatrix} \\ &+ \begin{bmatrix} 0 & 0 & 0 \\ 2\lambda_1 \bar{k}_{21}(x,1) & 0 & 0 \\ 2\lambda_1 \bar{k}_{31}(x,1) & 2\lambda_2 \bar{k}_{32}(x,1) & 0\end{bmatrix} \\ &+ \int_x^1 \begin{bmatrix} 2\lambda_1\Big(\bar{M}_{12}(x,\xi)\bar{k}_{21}(\xi,1) & & \\ \quad +\bar{M}_{13}(x,\xi)\bar{k}_{31}(\xi,1)\Big) & 2\lambda_2 \bar{M}_{13}(x,\xi)\bar{k}_{32}(\xi,1) & 0 \\ 2\lambda_1\Big(\bar{M}_{22}(x,\xi)\bar{k}_{21}(\xi,1) & & \\ \quad +\bar{M}_{23}(x,\xi)\bar{k}_{31}(\xi,1)\Big) & 2\lambda_2 \bar{M}_{23}(x,\xi)\bar{k}_{32}(\xi,1) & 0 \\ 2\lambda_1\Big(\bar{M}_{32}(x,\xi)\bar{k}_{21}(\xi,1) & & \\ \quad +\bar{M}_{33}(x,\xi)\bar{k}_{31}(\xi,1)\Big) & 2\lambda_2 \bar{M}_{33}(x,\xi)\bar{k}_{32}(\xi,1) & 0\end{bmatrix} d\xi \end{aligned} \tag{75a}$$

$$\begin{aligned}&\begin{bmatrix} \underline{P}^-_{11}(x) & \underline{P}^-_{12}(x) & \underline{P}^-_{13}(x) \\ \underline{P}^-_{21}(x) & \underline{P}^-_{22}(x) & \underline{P}^-_{23}(x) \\ \underline{P}^-_{31}(x) & \underline{P}^-_{32}(x) & \underline{P}^-_{33}(x)\end{bmatrix} = \\ &\quad \begin{bmatrix} 2\lambda_1 \bar{N}_{11}(x,1) & 2\lambda_2 \bar{N}_{12}(x,1) & 2\mu_1 \bar{N}_{13}(x,1) \\ 2\lambda_1 \bar{N}_{21}(x,1) & 2\lambda_2 \bar{N}_{22}(x,1) & 2\mu_1 \bar{N}_{23}(x,1) \\ 2\lambda_1 \bar{N}_{31}(x,1) & 2\lambda_2 \bar{N}_{32}(x,1) & 2\mu_1 \bar{N}_{33}(x,1)\end{bmatrix} \\ &+ \int_x^1 \begin{bmatrix} 2\lambda_1\Big(\bar{N}_{12}(x,\xi)\bar{k}_{21}(\xi,1) & & \\ \quad +\bar{N}_{13}(x,\xi)\bar{k}_{31}(\xi,1)\Big) & 2\lambda_2 \bar{N}_{13}(x,\xi)\bar{k}_{32}(\xi,1) & 0 \\ 2\lambda_1\Big(\bar{N}_{22}(x,\xi)\bar{k}_{21}(\xi,1) & & \\ \quad +\bar{N}_{23}(x,\xi)\bar{k}_{31}(\xi,1)\Big) & 2\lambda_2 \bar{N}_{23}(x,\xi)\bar{k}_{32}(\xi,1) & 0 \\ 2\lambda_1\Big(\bar{N}_{32}(x,\xi)\bar{k}_{21}(\xi,1) & & \\ \quad +\bar{N}_{33}(x,\xi)\bar{k}_{31}(\xi,1)\Big) & 2\lambda_2 \bar{N}_{33}(x,\xi)\bar{k}_{32}(\xi,1) & 0\end{bmatrix} d\xi. \end{aligned} \tag{75b}$$

The plots of the bilateral observer gains are shown in Figure 7.

4.2. Observer performance

The $2+1$ system is simulated in MATLAB for 8 seconds, using a first-order upwind finite difference scheme to approximate the

[3] Note that Π^+, Π^- are both equal to identity for this example.

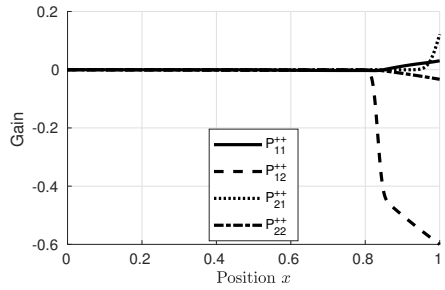

(a) Components P_{11}^{++}, P_{12}^{++}, P_{21}^{++} and P_{22}^{++}.

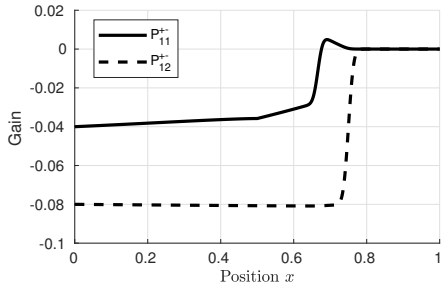

(b) Components P_{11}^{+-} and P_{12}^{+-}.

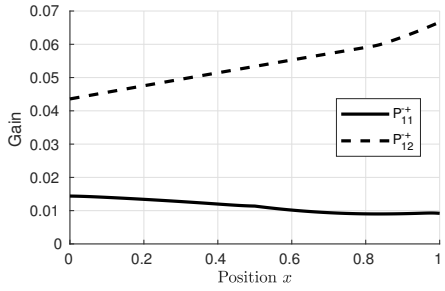

(c) Components P_{11}^{-+} and P_{21}^{-+}.

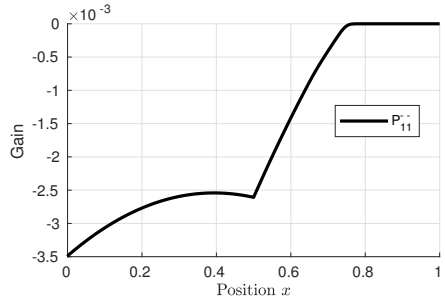

(d) Component P_{11}^{--}.

Figure 7: Bilateral minimum time observer gains P^{++}, P^{+-}, P^{-+} and P^{--}.

spatial derivatives and the `ode23` (Bogacki-Shampine, see [30]) solver in `MATLAB` to simulate the resultant ODE system. The states $u_1(x,t)$, $u_2(x,t)$ and $v_1(x,t)$ for the duration of the simulation are shown in Figure 8.

Applying the observer gains computed in Subsection 4.1, the three observers are implemented, all with zero initial conditions. To highlight the difference in convergence time between the three observers, the sum $\|\tilde{u}_1(t)\| + \|\tilde{u}_2(t)\| + \|\tilde{v}_1(t)\|$ of the L^2 norm of each of the error states for each observer is plotted as a solid line in Figure 9 while the vertical dashed lines represent the theoretical convergence time of the observer plotted with the corresponding colour. We see that the bilateral observer converges first, followed by the minimum time unilateral observer, and finally the non-minimum time unilateral observer.

Note that the estimation errors associated with all observers have slightly non-zero values when crossing the dashed lines corresponding to their respective convergence times. This is due to numerical errors from the first-order scheme used to calculate the integral kernels, giving slightly incorrect observer gains. The theory was proven for a continuous PDE system with the observer gains expressed exactly; however in practice this ideal scenario is generally not possible to reproduce perfectly and some approximation error must be expected.

5. Conclusion

We have shown an alternative way of deriving an $n+m$ minimum time bilateral observer than the one presented in [11]. Along the way, a unilateral minimum time observer for $n+m$ systems is derived, which was done by making the target system from [10] converge in minimum time with the help of a Fredholm transformation as in [25]. From this observer design, an observer using pointwise in-domain sensing was also derived. The observers using bilateral or in-domain sensing were shown to converge within the theoretical lower convergence bound from [7] for observers using both boundary measurements. As was noted in [26], some of the ideas considered there for control design could be applied to the design of bilateral observers. Indeed, as was demonstrated in [9] for 2×2 systems, this paper shows that the trick of domain folding is also applicable for bilateral observer design of $n+m$ systems. As future work, it would be interesting to investigate the applicability of domain folding to the design of observers for other classes of PDE systems.

References

[1] J.-M. Coron, R. Vazquez, M. Krstic, G. Bastin, Local exponential h^2 stabilization of a 2×2 quasilinear hyperbolic system using backstepping, SIAM Journal on Control and Optimization 51 (3) (2013) 2005–2035.

[2] G. Bastin, J.-M. Coron, Stability and boundary stabilization of 1-D hyperbolic systems, Vol. 88, Springer, 2016.

[3] O. M. Aamo, Disturbance rejection in 2×2 linear hyperbolic systems, IEEE Transactions on Automatic Control 58 (5) (2012) 1095–1106.

[4] D. G. Luenberger, Observing the state of a linear system, IEEE Transactions on Military Electronics 8 (2) (1964) 74–80.

[5] D. L. Russell, Controllability and stabilizability theory for linear partial differential equations: recent progress and open questions, SIAM Review 20 (4) (1978) 639–739.

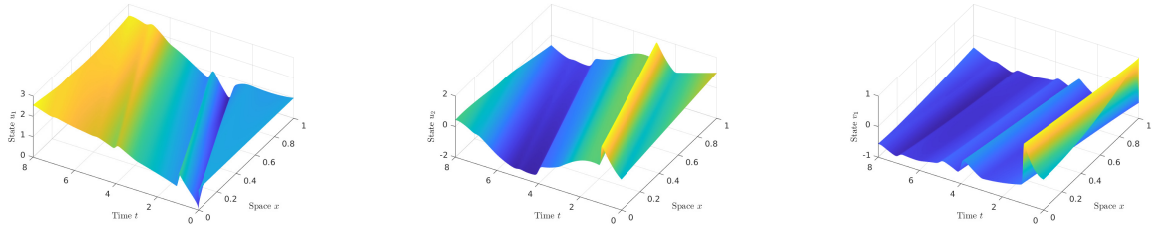

(a) State u_1. (b) State u_2. (c) State v_1.

Figure 8: States of system to be estimated.

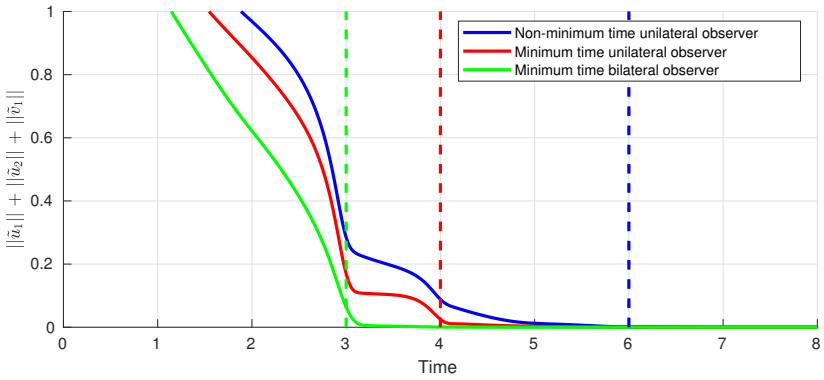

Figure 9: Sum of error norms $\|\tilde{u}_1\| + \|\tilde{u}_2\| + \|\tilde{v}_1\|$.

[6] N. Weck, A remark on controllability for symmetric hyperbolic systems in one space dimension, SIAM Journal on Control and Optimization 20 (1) (1982) 1–8.

[7] T. Li, B. Rao, Strong (weak) exact controllability and strong (weak) exact observability for quasilinear hyperbolic systems, Chinese Annals of Mathematics, Series B 31 (5) (2010) 723–742.

[8] J. Auriol, F. Di Meglio, Minimum time control of heterodirectional linear coupled hyperbolic PDEs, Automatica 71 (2016) 300–307.

[9] N. C. A. Wilhelmsen, H. Anfinsen, O. M. Aamo, Minimum time bilateral observer design for 2×2 linear hyperbolic systems, in: 2019 18th European Control Conference (ECC), IEEE, 2019, pp. 2325–2331.

[10] H. Anfinsen, O. M. Aamo, Disturbance rejection in general heterodirectional 1-D linear hyperbolic systems using collocated sensing and control, Automatica 76 (2017) 230–242.

[11] J. Auriol, F. Di Meglio, Two-sided boundary stabilization of heterodirectional linear coupled hyperbolic PDEs, IEEE Transactions on Automatic Control 63 (8) (2018) 2421–2436.

[12] C.-Z. Xu, G. Sallet, Exponential stability and transfer functions of processes governed by symmetric hyperbolic systems, ESAIM: Control, Optimisation and Calculus of Variations 7 (2002) 421–442.

[13] M. Gugat, M. Dick, G. Leugering, Gas flow in fan-shaped networks: Classical solutions and feedback stabilization, SIAM Journal on Control and Optimization 49 (5) (2011) 2101–2117.

[14] F. Di Meglio, U. J. F. Aarsnes, A distributed parameter systems view of control problems in drilling, IFAC-PapersOnLine 48 (6) (2015) 272–278.

[15] D. M. Boskovic, M. Krstic, W. Liu, Boundary control of an unstable heat equation via measurement of domain-averaged temperature, IEEE Transactions on Automatic Control 46 (12) (2001) 2022–2028.

[16] W. Liu, Boundary feedback stabilization of an unstable heat equation, SIAM Journal on Control and Optimization 42 (3) (2003) 1033–1043.

[17] A. Smyshlyaev, M. Krstic, Backstepping observers for a class of parabolic PDEs, Systems & Control Letters 54 (7) (2005) 613–625.

[18] V. T. Haimo, Finite time controllers, SIAM Journal on Control and Optimization 24 (4) (1986) 760–770.

[19] X. Huang, W. Lin, B. Yang, Global finite-time stabilization of a class of uncertain nonlinear systems, Automatica 41 (5) (2005) 881–888.

[20] P. Krishnamurthy, F. Khorrami, M. Krstic, Robust output-feedback prescribed-time stabilization of a class of nonlinear strict-feedback-like systems, in: 2019 18th European Control Conference (ECC), IEEE, 2019, pp. 1148–1153.

[21] J.-M. Coron, H.-M. Nguyen, Null controllability and finite time stabilization for the heat equations with variable coefficients in space in one dimension via backstepping approach, Archive for Rational Mechanics and Analysis 225 (3) (2017) 993–1023.

[22] D. Steeves, M. Krstic, R. Vazquez, Prescribed-time stabilization of reaction-diffusion equation by output feedback, in: 2019 American Control Conference (ACC), IEEE, 2019, pp. 2570–2575.

[23] D. Steeves, L. Camacho-Solorio, M. Krstic, Boundary prescribed–time stabilization of a pair of coupled reaction–diffusion equations, in: 2020 American Control Conference (ACC), IEEE, 2020, pp. 812–817.

[24] R. Vazquez, M. Krstic, J.-M. Coron, Backstepping boundary stabilization and state estimation of a 2×2 linear hyperbolic system, in: 2011 50th IEEE Conference on Decision and Control and European Control Conference (CDC-ECC), IEEE, 2011, pp. 4937–4942.

[25] J.-M. Coron, L. Hu, G. Olive, Finite-time boundary stabilization of general linear hyperbolic balance laws via Fredholm backstepping transformation, Automatica 84 (2017) 95–100.

[26] R. Vazquez, M. Krstic, Bilateral boundary control of one-dimensional first-and second-order PDEs using infinite-dimensional backstepping, in: 2016 IEEE 55th Conference on Decision and Control (CDC), IEEE, 2016, pp. 537–542.

[27] R. F. Curtain, H. Zwart, An introduction to infinite-dimensional linear systems theory, Vol. 21, Springer Science & Business Media, 2012.

[28] L. Hu, F. Di Meglio, R. Vazquez, M. Krstic, Control of homodirectional and general heterodirectional linear coupled hyperbolic PDEs, IEEE Transactions on Automatic Control 61 (11) (2016) 3301–3314.

[29] H. Anfinsen, O. M. Aamo, Adaptive control of hyperbolic PDEs, Springer, 2019.

[30] P. Bogacki, L. F. Shampine, A 3 (2) pair of runge-kutta formulas, Applied Mathematics Letters 2 (4) (1989) 321–325.

Appendix A. Kernel equations for simulation

Appendix A.1. Kernels for unilateral observers

The equations for the matrix-valued kernels M, N that are implemented in `MATLAB` to calculate the unilateral observer gains can be split into two seperate groups of three PDEs. The first group, consisting of M_{11}, M_{21} and N_{11} is described by

$$\lambda_1 M_{11,x}(x,\xi) + \lambda_1 M_{11,\xi}(x,\xi) = \sigma_{12}^{++}(x) M_{21}(x,\xi) + \sigma_{11}^{+-}(x) N_{11}(x,\xi) \quad \text{(A.1a)}$$

$$\lambda_2 M_{21,x}(x,\xi) + \lambda_1 M_{21,\xi}(x,\xi) = \sigma_{21}^{++}(x) M_{11}(x,\xi) + \sigma_{21}^{+-}(x) N_{11}(x,\xi) \quad \text{(A.1b)}$$

$$-\mu_1 N_{11,x}(x,\xi) + \lambda_1 N_{11,\xi}(x,\xi) = \sigma_{11}^{-+}(x) M_{11}(x,\xi) + \sigma_{12}^{-+}(x) M_{21}(x,\xi) \quad \text{(A.1c)}$$

with boundaries

$$M_{11}(0,\xi) = q_{11} N_{11}(0,\xi) \quad \text{(A.2a)}$$

$$M_{21}(x,1) = \frac{\sigma_{21}^{++}(x)}{\lambda_1 - \lambda_2} \quad \text{(A.2b)}$$

$$M_{21}(x,x) = \frac{\sigma_{21}^{++}(x)}{\lambda_1 - \lambda_2} \quad \text{(A.2c)}$$

$$N_{11}(x,x) = \frac{\sigma_{11}^{-+}(x)}{\lambda_1 + \mu_1} \quad \text{(A.2d)}$$

Likewise, the second group, for M_{12}, M_{22} and N_{12}, reads

$$\lambda_1 M_{12,x}(x,\xi) + \lambda_2 M_{12,\xi}(x,\xi) = \sigma_{12}^{++}(x) M_{22}(x,\xi) + \sigma_{11}^{+-}(x) N_{12}(x,\xi) \quad \text{(A.3a)}$$

$$\lambda_2 M_{22,x}(x,\xi) + \lambda_2 M_{22,\xi}(x,\xi) = \sigma_{21}^{++}(x) M_{12}(x,\xi) + \sigma_{21}^{+-}(x) N_{12}(x,\xi) \quad \text{(A.3b)}$$

$$-\mu_1 N_{12,x}(x,\xi) + \lambda_2 N_{12,\xi}(x,\xi) = \sigma_{11}^{-+}(x) M_{12}(x,\xi) + \sigma_{12}^{-+}(x) M_{22}(x,\xi) \quad \text{(A.3c)}$$

with boundaries

$$M_{12}(0,\xi) = q_{11} N_{12}(0,\xi) \quad \text{(A.4a)}$$

$$M_{12}(x,x) = \frac{\sigma_{12}^{++}(x)}{\lambda_2 - \lambda_1} \quad \text{(A.4b)}$$

$$M_{22}(0,\xi) = q_{21} N_2(0,\xi) \quad \text{(A.4c)}$$

$$N_{12}(x,x) = \frac{\sigma_{12}^{-+}(x)}{\lambda_2 + \mu_1}. \quad \text{(A.4d)}$$

To compute the minimum time unilateral observer gains, in addition to M, N, the lower triangular matrix-valued kernel K, with k_{21} as its only non-zero element needs to be solved. The equations for k_{21} reads

$$\lambda_2 k_{21,x}(x,\xi) + \lambda_1 k_{21,\xi}(x,\xi) = 0 \quad \text{(A.5)}$$

and has boundary conditions

$$k_{21}(x,0) = 0 \quad \text{(A.6a)}$$

$$k_{21}(0,\xi) = q_{21} N_{11}(0,\xi) - M_{21}(0,\xi). \quad \text{(A.6b)}$$

As it depends on the solution to N_{11} and M_{21}, these must be solved before K_{21}.

Appendix A.2. Kernels for bilateral observer

Applying the transformation T given in (44), with $x_s = \frac{1}{2}$, to the example in Section 4, a system (46) for $n = m = 3$ is obtained. Expressed in terms of the original coefficients, the new system has transport speeds

$$\overline{\Lambda}^{+} = \begin{bmatrix} 2\lambda_1 & 0 & 0 \\ 0 & 2\lambda_2 & 0 \\ 0 & 0 & 2\mu_1 \end{bmatrix}, \qquad \overline{\Lambda}^{-} = \begin{bmatrix} 2\lambda_1 & 0 & 0 \\ 0 & 2\lambda_2 & 0 \\ 0 & 0 & 2\mu_1 \end{bmatrix},$$

in-domain coupling coefficients

$$\overline{\Sigma}^{++}(x) = \begin{bmatrix} 0 & \sigma_{12}^{++}(0.5(1+x)) & 0 \\ \sigma_{21}^{++}(0.5(1+x)) & 0 & 0 \\ 0 & 0 & 0 \end{bmatrix},$$

$$\overline{\Sigma}^{+-}(x) = \begin{bmatrix} 0 & 0 & \sigma_{11}^{+-}(0.5(1+x)) \\ 0 & 0 & \sigma_{21}^{+-}(0.5(1+x)) \\ \sigma_{11}^{-+}(0.5(1-x)) & \sigma_{12}^{-+}(0.5(1-x)) & 0 \end{bmatrix},$$

$$\overline{\Sigma}^{-+}(x) = \begin{bmatrix} 0 & 0 & \sigma_{11}^{+-}(0.5(1-x)) \\ 0 & 0 & \sigma_{21}^{+-}(0.5(1-x)) \\ \sigma_{11}^{-+}(0.5(1+x)) & \sigma_{12}^{-+}(0.5(1+x)) & 0 \end{bmatrix},$$

$$\overline{\Sigma}^{--}(x) = \begin{bmatrix} 0 & \sigma_{12}^{++}(0.5(1-x)) & 0 \\ \sigma_{21}^{++}(0.5(1-x)) & 0 & 0 \\ 0 & 0 & 0 \end{bmatrix},$$

boundary condition matrices

$$\bar{Q}_0 = \begin{bmatrix} 1 & 0 & 0 \\ 0 & 1 & 0 \\ 0 & 0 & 1 \end{bmatrix}, \qquad \bar{R}_1 = \begin{bmatrix} 0 & 0 & q_{11} \\ 0 & 0 & q_{21} \\ \rho_{11} & \rho_{12} & 0 \end{bmatrix},$$

and I/O signals

$$\bar{y}(t) := \begin{bmatrix} y_{11}(t) \\ y_{12}(t) \\ y_0(t) \end{bmatrix}, \qquad \bar{U}(t) := \begin{bmatrix} U_{01}(t) \\ U_{02}(t) \\ U_{11}(t) \end{bmatrix}.$$

Substituting these coefficients into the kernel equations (14)–(15), one obtains three sets of six coupled PDEs that are solved in `MATLAB`.

The first set, which are equations for $\bar{M}_{11}$, $\bar{M}_{21}$, $\bar{M}_{31}$, $\bar{N}_{11}$, $\bar{N}_{21}$, $\bar{N}_{31}$ read

$$2\lambda_1 \bar{M}_{11,x}(x,\xi) + 2\lambda_1 \bar{M}_{11,\xi}(x,\xi) = \sigma_{12}^{++}(0.5(1+x)) \bar{M}_{21}(x,\xi) + \sigma_{11}^{+-}(0.5(1+x)) \bar{N}_{31}(x,\xi) \quad \text{(A.7a)}$$

$$-2\lambda_2 \bar{M}_{21,x}(x,\xi) - 2\lambda_1 \bar{M}_{21,\xi}(x,\xi) = -\sigma_{21}^{++}(0.5(1+x)) \bar{M}_{11}(x,\xi) - \sigma_{21}^{+-}(0.5(1+x)) \bar{N}_{31}(x,\xi) \quad \text{(A.7b)}$$

$$-2\mu_1 \bar{M}_{31,x}(x,\xi) - 2\lambda_1 \bar{M}_{31,\xi}(x,\xi) = -\sigma_{11}^{-+}(0.5(1-x)) \bar{N}_{11}(x,\xi) - \sigma_{12}^{-+}(0.5(1-x)) \bar{N}_{21}(x,\xi) \quad \text{(A.7c)}$$

$$-2\lambda_1 \bar{N}_{11,x}(x,\xi) + 2\lambda_1 \bar{N}_{11,\xi}(x,\xi) = \sigma_{11}^{+-}(0.5(1-x)) \bar{M}_{31}(x,\xi) + \sigma_{12}^{++}(0.5(1-x)) \bar{N}_{21}(x,\xi) \quad \text{(A.7d)}$$

$$-2\lambda_2 \bar{N}_{21,x}(x,\xi) + 2\lambda_1 \bar{N}_{21,\xi}(x,\xi) = \sigma_{21}^{+-}(0.5(1-x)) \bar{M}_{31}(x,\xi)$$

$$+ \sigma_{21}^{++}(0.5(1-x))\bar{N}_{11}(x,\xi) \tag{A.7e}$$

$$-2\mu_1\bar{N}_{31,x}(x,\xi) + 2\lambda_1\bar{N}_{31,\xi}(x,\xi) = \sigma_{11}^{-+}(0.5(1+x))\bar{M}_{11}(x,\xi) + \sigma_{12}^{-+}(0.5(1+x))\bar{M}_{21}(x,\xi) \tag{A.7f}$$

and have boundary conditions

$$\bar{M}_{11}(0,\xi) = \bar{N}_{11}(0,\xi) \tag{A.8a}$$

$$\bar{M}_{21}(x,x) = \frac{\sigma_{21}^{++}(0.5(1+x))}{2(\lambda_1-\lambda_2)} \tag{A.8b}$$

$$\bar{M}_{21}(x,1) = \frac{\sigma_{21}^{++}(0.5(1+x))}{2(\lambda_2-\lambda_1)} \tag{A.8c}$$

$$\bar{M}_{31}(x,x) = 0 \tag{A.8d}$$

$$\bar{M}_{31}(x,1) = 0 \tag{A.8e}$$

$$\bar{N}_{11}(x,x) = 0 \tag{A.8f}$$

$$\bar{N}_{21}(x,x) = 0 \tag{A.8g}$$

$$\bar{N}_{31}(x,x) = \frac{\sigma_{11}^{-+}(0.5(1+x))}{2(\mu_1+\lambda_1)} \tag{A.8h}$$

From the boundary conditions, we find that $\bar{M}_{31}(x,\xi) = 0$, $\bar{N}_{11}(x,\xi) = 0$ and $\bar{N}_{21}(x,\xi) = 0$ for all $(x,\xi) \in \mathcal{T}$.

Likewise, for $\bar{M}_{12}$, $\bar{M}_{22}$, $\bar{M}_{32}$, $\bar{N}_{12}$, $\bar{N}_{22}$, $\bar{N}_{32}$ one has

$$2\lambda_1\bar{M}_{12,x}(x,\xi) + 2\lambda_2\bar{M}_{12,\xi}(x,\xi) = \sigma_{12}^{++}(0.5(1+x))\bar{M}_{22}(x,\xi) + \sigma_{11}^{+-}(0.5(1+x))\bar{N}_{32}(x,\xi) \tag{A.9a}$$

$$2\lambda_2\bar{M}_{22,x}(x,\xi) + 2\lambda_2\bar{M}_{22,\xi}(x,\xi) = \sigma_{21}^{++}(0.5(1+x))\bar{M}_{12}(x,\xi) + \sigma_{21}^{+-}(0.5(1+x))\bar{N}_{32}(x,\xi) \tag{A.9b}$$

$$-2\mu_1\bar{M}_{32,x}(x,\xi) - 2\lambda_2\bar{M}_{32,\xi}(x,\xi) = -\sigma_{11}^{-+}(0.5(1-x))\bar{N}_{12}(x,\xi) - \sigma_{12}^{-+}(0.5(1-x))\bar{N}_{22}(x,\xi) \tag{A.9c}$$

$$-2\lambda_1\bar{N}_{12,x}(x,\xi) + 2\lambda_2\bar{N}_{12,\xi}(x,\xi) = \sigma_{11}^{+-}(0.5(1-x))\bar{M}_{32}(x,\xi) + \sigma_{12}^{++}(0.5(1-x))\bar{N}_{22}(x,\xi) \tag{A.9d}$$

$$-2\lambda_2\bar{N}_{22,x}(x,\xi) + 2\lambda_2\bar{N}_{22,\xi}(x,\xi) = \sigma_{21}^{+-}(0.5(1-x))\bar{M}_{32}(x,\xi) + \sigma_{21}^{++}(0.5(1-x))\bar{N}_{12}(x,\xi) \tag{A.9e}$$

$$-2\mu_1\bar{N}_{32,x}(x,\xi) + 2\lambda_2\bar{N}_{32,\xi}(x,\xi) = \sigma_{11}^{-+}(0.5(1+x))\bar{M}_{12}(x,\xi) + \sigma_{12}^{-+}(0.5(1+x))\bar{M}_{22}(x,\xi) \tag{A.9f}$$

with boundary conditions

$$\bar{M}_{12}(x,x) = \frac{\sigma_{12}^{++}(0.5(1+x))}{2(\lambda_2-\lambda_1)} \tag{A.10a}$$

$$\bar{M}_{12}(0,\xi) = \bar{N}_{12}(0,\xi) \tag{A.10b}$$

$$\bar{M}_{22}(0,\xi) = \bar{N}_{22}(0,\xi) \tag{A.10c}$$

$$\bar{M}_{32}(x,x) = 0 \tag{A.10d}$$

$$\bar{M}_{32}(x,1) = 0 \tag{A.10e}$$

$$\bar{N}_{12}(x,x) = 0 \tag{A.10f}$$

$$\bar{N}_{22}(x,x) = 0 \tag{A.10g}$$

$$\bar{N}_{32}(x,x) = \frac{\sigma_{12}^{-+}(0.5(1+x))}{2(\mu_1+\lambda_2)}. \tag{A.10h}$$

Also here we find that $\bar{M}_{32}(x,\xi) = 0$, $\bar{N}_{12}(x,\xi) = 0$ and $\bar{N}_{22}(x,\xi) = 0$.

The third group of equations, for $\bar{M}_{13}$, $\bar{M}_{23}$, $\bar{M}_{33}$, $\bar{N}_{13}$, $\bar{N}_{23}$, $\bar{N}_{33}$, is

$$2\lambda_1\bar{M}_{13,x}(x,\xi) + 2\mu_1\bar{M}_{13,\xi}(x,\xi) = \sigma_{12}^{++}(0.5(1+x))\bar{M}_{23}(x,\xi) + \sigma_{11}^{+-}(0.5(1+x))\bar{N}_{33}(x,\xi) \tag{A.11a}$$

$$2\lambda_2\bar{M}_{23,x}(x,\xi) + 2\mu_1\bar{M}_{23,\xi}(x,\xi) = \sigma_{21}^{++}(0.5(1+x))\bar{M}_{13}(x,\xi) + \sigma_{21}^{+-}(0.5(1+x))\bar{N}_{33}(x,\xi) \tag{A.11b}$$

$$2\mu_1\bar{M}_{33,x}(x,\xi) + 2\mu_1\bar{M}_{33,\xi}(x,\xi) = \sigma_{11}^{-+}(0.5(1-x))\bar{N}_{13}(x,\xi) + \sigma_{12}^{-+}(0.5(1-x))\bar{N}_{23}(x,\xi) \tag{A.11c}$$

$$-2\lambda_1\bar{N}_{13,x}(x,\xi) + 2\mu_1\bar{N}_{13,\xi}(x,\xi) = \sigma_{11}^{+-}(0.5(1-x))\bar{M}_{33}(x,\xi) + \sigma_{12}^{++}(0.5(1-x))\bar{N}_{23}(x,\xi) \tag{A.11d}$$

$$-2\lambda_2\bar{N}_{23,x}(x,\xi) + 2\mu_1\bar{N}_{23,\xi}(x,\xi) = \sigma_{21}^{+-}(0.5(1-x))\bar{M}_{33}(x,\xi) + \sigma_{21}^{++}(0.5(1-x))\bar{N}_{13}(x,\xi) \tag{A.11e}$$

$$-2\mu_1\bar{N}_{33,x}(x,\xi) + 2\mu_1\bar{N}_{33,\xi}(x,\xi) = \sigma_{11}^{-+}(0.5(1+x))\bar{M}_{13}(x,\xi) + \sigma_{12}^{-+}(0.5(1+x))\bar{M}_{23}(x,\xi) \tag{A.11f}$$

with boundary conditions

$$\bar{M}_{13}(x,x) = 0 \tag{A.12a}$$

$$\bar{M}_{13}(0,\xi) = \bar{N}_{13}(0,\xi) \tag{A.12b}$$

$$\bar{M}_{23}(x,x) = 0 \tag{A.12c}$$

$$\bar{M}_{23}(0,\xi) = \bar{N}_{23}(0,\xi) \tag{A.12d}$$

$$\bar{M}_{33}(0,\xi) = \bar{N}_{33}(0,\xi) \tag{A.12e}$$

$$\bar{N}_{13}(x,x) = \frac{\sigma_{11}^{+-}(0.5(1-x))}{2(\mu_1+\lambda_1)} \tag{A.12f}$$

$$\bar{N}_{23}(x,x) = \frac{\sigma_{21}^{+-}(0.5(1-x))}{2(\mu_1+\lambda_2)} \tag{A.12g}$$

$$\bar{N}_{33}(x,x) = 0. \tag{A.12h}$$

In addition to the matrix-valued kernel equations $\bar{M}$, $\bar{N}$, the strictly lower triangular 3×3 matrix-valued kernel $\bar{K}$, which has three non-zero elements $\bar{k}_{21}$, $\bar{k}_{31}$ and $\bar{k}_{32}$ must be solved. These are governed by the system

$$2\lambda_2\bar{k}_{21,x}(x,\xi) + 2\lambda_1\bar{k}_{21,\xi}(x,\xi) = 0 \tag{A.13a}$$

$$2\mu_1\bar{k}_{32,x}(x,\xi) + 2\lambda_2\bar{k}_{32,\xi}(x,\xi) = 0 \tag{A.13b}$$

$$2\mu_1\bar{k}_{31,x}(x,\xi) + 2\lambda_1\bar{k}_{31,\xi}(x,\xi) = -2\lambda_2\bar{k}_{32}(x,1)\bar{k}_{21}(1,\xi) \tag{A.13c}$$

with boundary conditions

$$\bar{k}_{21}(0,\xi) = \bar{N}_{21}(0,\xi) - \bar{M}_{21}(0,\xi) \tag{A.14a}$$
$$\bar{k}_{21}(x,0) = 0 \tag{A.14b}$$
$$\bar{k}_{32}(0,\xi) = \bar{N}_{32}(0,\xi) - \bar{M}_{32}(0,\xi) \tag{A.14c}$$
$$\bar{k}_{32}(x,0) = 0 \tag{A.14d}$$
$$\bar{k}_{31}(0,\xi) = \bar{N}_{31}(0,\xi) - \bar{M}_{31}(0,\xi) + \int_0^1 \left(\bar{N}_{32}(0,s) - \bar{M}_{32}(0,s)\right)\bar{k}_{21}(s,\xi)ds \tag{A.14e}$$
$$\bar{k}_{31}(x,0) = 0 \tag{A.14f}$$

The solutions to $\bar{K}$ depends on the solutions to $\bar{M}$, $\bar{N}$ and hence the latter must be solved first. Also, as illustrated in Figure 3, the solution to $\bar{k}_{31}$ depends on the solutions to $\bar{k}_{21}$, $\bar{k}_{32}$, so these two must be computed before $\bar{k}_{31}$ is calculated.

Appendix B. Definition of weak solutions

We define here what is meant by weak solutions to the plant (1) and error system (20). The definition of solutions to the observer (11), as well as all systems considered in Section 3, follow consequently from the definitions herein.

Appendix B.1. Weak solutions of (1)

For any given $\tau > 0$, multiply the dynamics (1a)–(1b) on the left by test function $\varphi^\top = [(\varphi^+)^\top\ (\varphi^-)^\top]$, where $\varphi^+ : [0,1]\times[0,\tau] \mapsto \mathbb{R}^n$, $\varphi^- : [0,1]\times[0,\tau] \mapsto \mathbb{R}^m$, integrate by parts over $(0,1)\times(0,\tau)$ and substitute in the boundary conditions (1c)–(1d) to obtain

$$\begin{aligned}
0 = &\int_0^1 \left(\varphi^+(x,\tau)^\top u(x,\tau) + \varphi^-(x,\tau)^\top v(x,\tau)\right)dx \\
&- \int_0^1 \left(\varphi^+(x,0)^\top u_0(x) + \phi^-(x,0)^\top v_0(x)\right)dx \\
&+ \int_0^\tau \left(\varphi^+(1,t)^\top\Lambda^+ - \varphi^-(1,t)^\top\Lambda^- R_1\right)u(1,t)dt \\
&+ \int_0^\tau \left(\varphi^-(0,t)^\top\Lambda^- - \varphi^+(0,t)^\top\Lambda^+ Q_0\right)v(0,t)dt \\
&- \int_0^\tau \left(\varphi^-(1,t)^\top\Lambda^- U_1(t) + \varphi^+(0,t)^\top U_0(t)\right)dt \\
&- \int_0^1\int_0^\tau \left((\varphi_t^+)^\top + (\varphi_x^+)^\top\Lambda^+ + (\varphi^+)^\top\Sigma^{++}\right. \\
&\left.+ (\varphi^-)^\top\Sigma^{-+}\right)u(x,t)dtdx - \int_0^1\int_0^\tau \left((\varphi_t^-)^\top - (\varphi_x^-)^\top\Lambda^-\right. \\
&\left.+ (\varphi^+)^\top\Sigma^{+-} + (\varphi^-)^\top\Sigma^{--}\right)v(x,t)dtdx.
\end{aligned} \tag{B.1}$$

Letting the initial conditions in (1e)–(1f) satisfy $u_0 \in L^2((0,1);\mathbb{R}^n)$, $v_0 \in L^2((0,1);\mathbb{R}^m)$, it can be shown that (see the proof of Theorem A.4 in [2]) for every $\tau > 0$ and $\varphi^+ \in C^1([0,1]\times[0,\tau];\mathbb{R}^n), \varphi^- \in C^1([0,1]\times[0,\tau];\mathbb{R}^m)$ satisfying

$$\varphi^+(1,t) = (\Lambda^+)^{-1}R_1^\top\Lambda^-\varphi^-(1,t) \tag{B.2a}$$
$$\varphi^-(0,t) = (\Lambda^-)^{-1}Q_0^\top\Lambda^+\varphi^+(0,t), \tag{B.2b}$$

the system (1) has a unique (weak) solution $u \in C^0([0,\infty);L^2((0,1);\mathbb{R}^n))$, $v \in C^0([0,\infty);L^2((0,1);\mathbb{R}^m))$, satisfying

$$\begin{aligned}
&\int_0^1 \left(\varphi^+(x,\tau)^\top u(x,\tau) + \varphi^-(x,\tau)^\top v(x,\tau)\right)dx \\
&\quad - \int_0^1 \left(\varphi^+(x,0)^\top u_0(x) + \varphi^-(x,0)^\top v_0(x)\right)dx \\
&= \int_0^1\int_0^\tau \left((\varphi_t^+)^\top + (\varphi_x^+)^\top\Lambda^+ + (\varphi^+)^\top\Sigma^{++}\right. \\
&\quad \left.+ (\varphi^-)^\top\Sigma^{-+}\right)u(x,t)dtdx + \int_0^1\int_0^\tau \left((\varphi_t^-)^\top - (\varphi_x^-)^\top\Lambda^-\right. \\
&\quad \left.+ (\varphi^+)^\top\Sigma^{+-} + (\varphi^-)^\top\Sigma^{--}\right)v(x,t)dtdx \\
&\quad + \int_0^\tau (\varphi^-(1,t)^\top\Lambda^- U_1(t) + \varphi^+(0,t)^\top U_0(t))dt.
\end{aligned} \tag{B.3}$$

Appendix B.2. Weak solutions of (20)

Multiply the dynamics (20a)–(20b) on the left by a test function $\psi^\top = [(\psi^+)^\top\ (\psi^-)^\top]$, where $\psi^+ : [0,1]\times[0,\tau] \mapsto \mathbb{R}^n$, $\psi^- : [0,1]\times[0,\tau] \mapsto \mathbb{R}^m$, integrate by parts and substitute in boundary conditions (20c)–(20d). Letting the initial conditions in (20e)–(20f) satisfy $\tilde{u}_0 \in L^2((0,1);\mathbb{R}^n)$ and $\tilde{v}_0 \in L^2((0,1);\mathbb{R}^m)$, it can be shown that (see the proof of Theorem A.4 in [2]) for every $\tau > 0$ and $\psi^+ \in C^1([0,1]\times[0,\tau];\mathbb{R}^n), \psi^- \in C^1([0,1]\times[0,\tau];\mathbb{R}^m)$ satisfying

$$\psi^+(1,t) = (\Lambda^+)^{-1}\int_0^1 \left(P^+(x)^\top\psi^+(x,t) + P^-(x)^\top\psi^-(x,t)\right)dx \tag{B.4a}$$
$$\psi^-(0,t) = (\Lambda^-)^{-1}Q_0\Lambda^+\psi^+(0,t) \tag{B.4b}$$

the error system (20) has a unique (weak) solution $\tilde{u} \in C^0([0,\infty);L^2((0,1);\mathbb{R}^n))$, $\tilde{v} \in C^0([0,\infty);L^2((0,1);\mathbb{R}^m))$, satisfying

$$\begin{aligned}
&\int_0^1 \left(\psi^+(x,\tau)^\top\tilde{u}(x,\tau) + \psi^-(x,\tau)^\top\tilde{v}(x,\tau)\right)dx \\
&\quad - \int_0^1 \left(\psi^+(x,0)^\top\tilde{u}_0(x) + \psi^-(x,0)^\top\tilde{v}_0(x)\right)dx \\
&= \int_0^1\int_0^\tau \left((\psi_t^+)^\top + (\psi_x^+)^\top\Lambda^+ + (\psi^+)^\top\Sigma^{++}\right. \\
&\quad \left.+ (\psi^-)^\top\Sigma^{-+}\right)\tilde{u}(x,t)dtdx + \int_0^1\int_0^\tau \left((\psi_t^-)^\top - (\psi_x^-)^\top\Lambda^-\right. \\
&\quad \left.+ (\psi^+)^\top\Sigma^{+-} + (\psi^-)^\top\Sigma^{--}\right)\tilde{v}(x,t)dtdx.
\end{aligned} \tag{B.5}$$